CERN-PH-TH/2004-051
MC-TH-2004-03
hep-ph/0404167
April 2004

LHC Signatures of Resonant CP Violation in a Minimal Supersymmetric Higgs Sector

John Ellis[a], Jae Sik Lee[b] and Apostolos Pilaftsis[b]

[a] *Theory Division, Physics Department, CERN, CH-1211 Geneva 23, Switzerland*

[b] *Department of Physics and Astronomy, University of Manchester Manchester M13 9PL, United Kingdom*

ABSTRACT

We present the general formalism for studying CP-violating phenomena in the production, mixing and decay of a coupled system of CP-violating neutral Higgs bosons at high-energy colliders. Considering the Minimal Supersymmetric Standard Model (MSSM) Higgs sector in which CP violation is radiatively induced by phases in the soft supersymmetry-breaking third-generation trilinear squark couplings and gaugino masses, we apply our formalism to neutral Higgs production via $\bar{b}b$, gg and W^+W^- collisions at the LHC. We discuss CP asymmetries in the longitudinal and transverse polarizations of $\tau^+\tau^-$ pairs. The signatures of CP violation are more prominent in the production via gg and W^+W^- than via $\bar{b}b$, and are resonantly enhanced when two (or all three) neutral Higgs bosons are nearly degenerate with mass differences comparable to their decay widths. Such scenarios occur naturally in the MSSM for values of $\tan\beta \gtrsim 5$ (30) and large (small) charged Higgs-boson masses. We analyze representative examples with large mixing between the three neutral Higgs bosons weighing about 120 GeV, that may exhibit observable CP asymmetries even as large as 80%.

1 Introduction

If supersymmetry (SUSY) turns out to be realized at low energies $\lesssim 1$ TeV [1], the following interesting questions will then arise: does SUSY make observable contributions to the violation of either flavour or CP? Even in the minimal supersymmetric extension of the Standard Model (MSSM), the soft SUSY-breaking sector may include about a hundred parameters that violate these symmetries. However, if one imposes flavour conservation on the soft SUSY-breaking parameters $m_0, m_{1/2}$ and A, and assumes that they are universal, then only two physical CP-violating phases remain: one in the gaugino masses $m_{1/2}$ and one in the trilinear couplings A.

These CP-violating phases may in principle be measured directly in the production cross sections and decay widths of sparticles at high-energy colliders [2,3], or indirectly via their radiative effect on the Higgs sector [4] [1]. The Higgs sector of the MSSM is affected at the one-loop level by the trilinear phase [4, 10, 11, 12, 13, 14, 16, 17, 15] and at the two-loop level by the gaugino mass phase [12, 13, 14, 15]. This loop-induced CP violation mixes the CP-even Higgses h, H with the CP-odd Higgs boson A. Many studies have been made of the masses and couplings of the resulting mixed-CP Higgs bosons $H_{1,2,3}$, and some of their phenomenological consequences for searches at LEP and future colliders have also been considered [18, 19, 20, 21, 22, 23, 24, 25, 26].

More complete studies of CP-violating Higgs bosons will require a careful treatment of the resonant mixing of multiple Higgs bosons that couple to the same initial and final states. In general, one could expect that the CP-violating mixing of the heavier MSSM Higgs bosons H, A may be more important than their mixings with the lightest CP-even Higgs boson h. However, non-negligible mixing among all three neutral Higgs states is also possible in a general CP-violating MSSM. Such a scenario naturally emerges from a parameter space where $\tan\beta$ is large, i.e. $\tan\beta \gtrsim 30$, and the charged Higgs bosons $H^\pm$ are relatively light with $M_{H^\pm} \lesssim 160$ GeV.

In this paper, we develop the general formalism for describing the dynamics that governs the production, mixing and decay of a coupled system of CP-violating neutral Higgs bosons. Our formalism makes use of the field-theoretic resummation approach developed in [27] to treat unstable particle-mixing transitions. Within the context of gauge theories, it is important that resummation approaches to unstable particles consistently maintain crucial field-theoretic properties, such as gauge invariance, analyticity and unitarity [28].

[1] Additional indirect constraints on the soft SUSY-breaking phases and the MSSM mass spectrum may be obtained from experimental limits on electric dipole moments (EDMs) [5,6,7] and B-meson observables [8, 9].

It has been shown in [28, 29] that all these properties are preserved within the framework of the Pinch Technique (PT) [30]. Here, using the PT, we compute the gauge-mediated diagonal as well as off-diagonal absorptive parts in the resummed Higgs-boson propagator matrix. Finally, an essential ingredient of our formalism is the inclusion of the CP-violating loop corrections in the production and decay vertices of the Higgs bosons.

We illustrate our general formalism for the coupled-channel $H_{1,2,3}$ mixing by explicit treatments of the production processes gg, $b\bar{b}$ [2] and $W^+W^- \to H_{1,2,3} \to \tau^+\tau^-$. These are the most important production mechanisms for neutral Higgs bosons at the LHC, while the decay channel that seems the most promising for studies of CP violation is that into $\tau^+\tau^-$ pairs. To quantify the genuine signatures of CP violation, we calculate CP asymmetries that are defined in terms of longitudinal and transverse polarizations of the $\tau^\pm$ leptons. When $\tan\beta$ is large and/or the charged Higgs boson mass is large, so that two or more Higgs bosons are nearly degenerate, even small CP-violating phases could induce sizeable CP-violating mixing. However, as we demonstrate, there are systematic cancellations due to CPT-preserving rescattering effects in the process $b\bar{b} \to H_{1,2,3} \to \tau^+\tau^-$ that suppress the CP-violating signatures in this case. There are no such cancellations in gg and $W^+W^- \to H_{1,2,3} \to \tau^+\tau^-$, which could have much larger CP asymmetries at the LHC. We analyze representative examples with large three-way mixing to show that these CP asymmetries might well exceed the 10% level and could even reach values up to 80%.

Although our predictions are obtained in the MSSM with explicit CP violation, it is important to stress that large CP-violating effects could also occur in a general CP-violating 2-Higgs-doublet model with a similar Higgs-boson mass spectrum. Our presentation is organized in such a way that the formalism may easily be extended to Higgs production at other colliders. For instance, our formalism can be applied to $\gamma\gamma$ colliders [25,32], which are analogous to gg collisions at the LHC, to $\mu^+\mu^-$ colliders [26], which have formal similarities with $b\bar{b}$ collisions at the LHC, and to WW-fusion and Higgsstrahlung processes at e^+e^- linear colliders [33].

Section 2 presents the general formalism for the coupled-channel analysis of Higgs bosons, including explicit formulae for the absorptive parts of the Higgs-boson propagator matrix and the vertex corrections. In Section 3, we apply the results of our formalism to the production channels $gg, b\bar{b}, W^+W^- \to \tau^+\tau^-$ at the LHC. In Section 4 we present numerical estimates of particular CP-violating MSSM scenarios that exhibit large CP asymmetries. Our numerical estimates are based on the Fortran code `CPsuperH` [34]. Finally, Section 5 contains our conclusions and discusses the prospects for pursuing studies of Higgs-sector

[2] We note that the $b\bar{b}$ fusion process may become the leading production channel at large $\tan\beta$ at the LHC, as has recently been shown in [31].

CP violation at future colliders beyond the LHC.

2 Formalism for Coupled-Channel Analyses of Higgs-Sector CP Violation

We consider situations where two or more MSSM Higgs bosons contribute simultaneously to the production of some fermion-antifermion pair whose polarization states can be measured. We treat explicitly the example of $H_{1,2,3} \to \tau^+\tau^-$, but the formalism could easily be adapted to other cases such as $t\bar{t}$, $\chi_i^+\chi_j^-$ or $\chi_i^0\chi_j^0$. There have been extensive discussions of the masses and couplings of MSSM Higgs bosons mixed by loop-induced CP violation [10, 11, 12, 13]. To account properly for the constraints that CPT invariance and unitarity imposes on the cross sections [27], we must consider the full off-shell propagator matrix for mixed MSSM Higgs bosons, including off-diagonal absorptive parts.

The absorptive part of the Higgs-boson propagator matrix receives contributions from loops of fermions, vector bosons, associated pairs of Higgs and vector bosons, Higgs-boson pairs, and sfermions:

$$\Im\mathrm{m}\widehat{\Pi}_{ij}(s) = \Im\mathrm{m}\widehat{\Pi}_{ij}^{ff}(s) + \Im\mathrm{m}\widehat{\Pi}_{ij}^{VV}(s) + \Im\mathrm{m}\widehat{\Pi}_{ij}^{HV}(s) + \Im\mathrm{m}\widehat{\Pi}_{ij}^{HH}(s) + \Im\mathrm{m}\widehat{\Pi}_{ij}^{\tilde{f}\tilde{f}}(s)\,. \qquad (2.1)$$

The contributions of the exchanges of the bottom and top quarks, τ leptons, neutralinos χ_i^0 and charginos χ_i^+ are summed in $\Im\mathrm{m}\widehat{\Pi}_{ij}^{ff}(s)$. The latter may conveniently be cast into the form

$$\begin{aligned}\Im\mathrm{m}\widehat{\Pi}_{ij}^{ff}(s) &= \frac{s}{8\pi}\sum_{f,f'=b,t,\tau,\tilde{\chi}^0,\tilde{\chi}^-} K_f(s)\, g_f^2 \Delta_{ff'} N_C^f \Big[(1-\kappa_f-\kappa_{f'})(g^S_{H_i\bar{f}'f}g^{S*}_{H_j\bar{f}'f} + g^P_{H_i\bar{f}'f}g^{P*}_{H_j\bar{f}'f}) \\ &\quad -2\sqrt{\kappa_f\kappa_{f'}}(g^S_{H_i\bar{f}'f}g^{S*}_{H_j\bar{f}'f} - g^P_{H_i\bar{f}'f}g^{P*}_{H_j\bar{f}'f})\Big]\,\lambda^{1/2}(1,\kappa_f,\kappa_{f'})\,\Theta\left(s-(m_f+m_{f'})^2\right), \qquad (2.2)\end{aligned}$$

where $K_{b,t}(s) \simeq 1+5.67\frac{\alpha_s(s)}{\pi}$, $\Delta_{ff'} = \delta_{ff'}$ $(f, f' = b, t, \tau)$, $\frac{4}{1+\delta_{ff'}}$ $(f, f' = \tilde{\chi}^0_{1,2,3,4})$, or 1 $(f, f' = \tilde{\chi}^-_{1,2})$, and $\lambda(x,y,z) = x^2+y^2+z^2-2(xy+yz+zx)$ with $\kappa_x \equiv m_x^2/s$. Here and subsequently, we follow the convention of `CPsuperH` [34] for the couplings of the Higgs bosons to fermions, vector bosons, Higgs bosons, and sfermions.

The vector-boson loop contributions are

$$\begin{aligned}\Im\mathrm{m}\widehat{\Pi}_{ij}^{VV}(s) &= \frac{g^2 g_{H_iVV} g_{H_jVV}\delta_V}{128\pi M_W^2}\beta_V\Big[-4M_V^2(2s-3M_V^2) \\ &\qquad +2M_V^2(M_{H_i}^2+M_{H_j}^2) + M_{H_i}^2 M_{H_j}^2\Big]\,\Theta(s-4M_V^2), \qquad (2.3)\end{aligned}$$

where $\beta_V = (1-4\kappa_V)^{1/2}$ and $\delta_W = 2$, $\delta_Z = 1$.

Correspondingly, the exchanges of Higgs and vector boson pairs give

$$\begin{aligned}\Im\mathrm{m}\widehat{\Pi}^{HV}_{ij}(s) &= \frac{g^2}{64\pi M_W^2}\sum_{k=1,2,3} g_{H_iH_kZ}g_{H_jH_kZ}\lambda^{1/2}(1,\kappa_Z,\kappa_{H_k})\left[-4sM_Z^2+(M_Z^2-M_{H_k}^2)^2\right.\\ &\quad\left.+(M_Z^2-M_{H_k}^2)(M_{H_i}^2+M_{H_j}^2)+M_{H_i}^2M_{H_j}^2\right]\Theta\left(s-(M_Z+M_{H_k})^2\right)\\ &+ \frac{g^2}{32\pi M_W^2}\Re\mathrm{e}(g_{H_iH^+W^-}g^*_{H_jH^+W^-})\lambda^{1/2}(1,\kappa_W,\kappa_{H^\pm})\left[-4sM_W^2+(M_W^2-M_{H^\pm}^2)^2\right.\\ &\quad\left.+(M_W^2-M_{H^\pm}^2)(M_{H_i}^2+M_{H_j}^2)+M_{H_i}^2M_{H_j}^2\right]\Theta\left(s-(M_W+M_{H^\pm})^2\right). \quad (2.4)\end{aligned}$$

In deriving (2.3) and (2.4), we apply the PT to the MSSM Higgs sector following a procedure very analogous to the one given in [35] for the SM Higgs sector. As a consequence, the PT self-energies $\Im\mathrm{m}\widehat{\Pi}^{VV}_{ij}(s)$ and $\Im\mathrm{m}\widehat{\Pi}^{VH}_{ij}(s)$ depend linearly on s at high energies. This differs crucially from the bad high-energy dependence $\propto s^2$ that one usually encounters when the Higgs-boson self-energies are calculated in the unitary gauge. In fact, if the Higgs-boson self-energies are embedded in a truly gauge-independent quantity such as the S-matrix element of a $2\to 2$ process, the badly high-energy-behaved s^2-dependent terms cancel against corresponding s^2 terms present in the vertices and boxes order by order in perturbation theory. In this context, PT provides a self-consistent approach to extract those s^2-dependent terms from boxes and vertices, thus giving rise to effective Higgs self-energies that are independent of the gauge-fixing parameter and s^2. More details on the PT may be found in [28, 29, 30, 35].

Finally, the contributions of the MSSM Higgs bosons and sfermions are

$$\Im\mathrm{m}\widehat{\Pi}^{HH}_{ij}(s) = \frac{v^2}{16\pi}\sum_{k\geq l=1,2,3}\frac{S_{ij;kl}}{1+\delta_{kl}}g_{H_iH_kH_l}g_{H_jH_kH_l}\lambda^{1/2}(1,\kappa_{H_k},\kappa_{H_l})\,\Theta\left(s-(M_{H_k}+M_{H_l})^2\right), \quad (2.5)$$

$$\Im\mathrm{m}\widehat{\Pi}^{\tilde{f}\tilde{f}}_{ij}(s) = \frac{v^2}{16\pi}\sum_{f=b,t,\tau}\sum_{k,l=1,2}N_C^f\,g_{H_i\tilde{f}_k^*\tilde{f}_l}g^*_{H_j\tilde{f}_k^*\tilde{f}_l}\lambda^{1/2}(1,\kappa_{\tilde{f}_k},\kappa_{\tilde{f}_l})\,\Theta\left(s-(M_{\tilde{f}_k}+M_{\tilde{f}_l})^2\right). \quad (2.6)$$

Note that the symmetry factor $S_{ij;kl}$ has to be calculated appropriately. When $i=j=1$ and $k=l=2$, for example, the symmetry factor for the squared self-coupling $g^2_{H_1H_2H_2}$ is $S_{11;22}=4$.

When considering any specific production process and decay channel, the Higgs-boson propagator matrix must be combined with the appropriate vertices, that themselves receive CP-violating loop corrections. Since the main decay channel we consider for the LHC is $\tau^+\tau^-$, and since many of the interesting Higgs production and other decay mechanisms also involve fermions such as $b\bar{b}$, we also summarize relevant aspects of the loop-induced corrections to the $H_{1,2,3}f\bar{f}$ vertices.

The exchanges of gluinos and charginos give finite loop-induced corrections to the $H_{1,2,3}b\bar{b}$ Yukawa coupling with the structure

$$h_b \;=\; \frac{\sqrt{2}m_b}{v\cos\beta}\,\frac{1}{1+(\delta h_b/h_b)+(\Delta h_b/h_b)\tan\beta}\,. \tag{2.7}$$

The $\tan\beta$-enhanced threshold correction $(\Delta h_b/h_b)$ has terms proportional to the strong coupling α_s and the top-quark Yukawa coupling $|h_t|^2$ which are given, for example, in [20]. In addition, there are contributions to $(\Delta h_b/h_b)$ coming from the exchanges of binos and winos which are proportional to the electromagnetic fine-structure constant $\alpha_{\rm em}$ [36]. Taking CP violation into account, these additional contributions read

$$\begin{aligned}
(\Delta h_b/h_b)_{\rm em} \;=\; & -\frac{\alpha_{\rm em}\mu^* M_2^*}{4\pi\, s_W^2}\Bigg[\,|U^{\tilde{t}}_{L1}|^2\, I(m^2_{\tilde{t}_1},|M_2|^2,|\mu|^2)\;+\;|U^{\tilde{t}}_{L2}|^2\, I(m^2_{\tilde{t}_2},|M_2|^2,|\mu|^2) \\
& +\frac{1}{2}\,|U^{\tilde{b}}_{L1}|^2\, I(m^2_{\tilde{b}_1},|M_2|^2,|\mu|^2)\;+\;\frac{1}{2}\,|U^{\tilde{b}}_{L2}|^2\, I(m^2_{\tilde{b}_2},|M_2|^2,|\mu|^2)\Bigg] \\
& -\frac{\alpha_{\rm em}\mu^* M_1^*}{12\pi c_W^2}\Bigg[\frac{1}{3}\, I(m^2_{\tilde{b}_1},m^2_{\tilde{b}_2},|M_1|^2)\;+\;\frac{1}{2}\,|U^{\tilde{b}}_{L1}|^2\, I(m^2_{\tilde{b}_1},|M_1|^2,|\mu|^2) \\
& +\frac{1}{2}\,|U^{\tilde{b}}_{L2}|^2\, I(m^2_{\tilde{b}_2},|M_1|^2,|\mu|^2)\;+\;|U^{\tilde{b}}_{R1}|^2\, I(m^2_{\tilde{b}_1},|M_1|^2,|\mu|^2) \\
& +|U^{\tilde{b}}_{R2}|^2\, I(m^2_{\tilde{b}_2},|M_1|^2,|\mu|^2)\Bigg]\,,
\end{aligned} \tag{2.8}$$

where

$$I(a,b,c) \;=\; \frac{ab\,\ln(a/b)\;+\;bc\,\ln(b/c)\;+\;ac\,\ln(c/a)}{(a-b)\,(b-c)\,(a-c)}\,. \tag{2.9}$$

We follow the convention of `CPsuperH` [34] for the mixing matrices of the stops $U^{\tilde{t}}$, sbottoms $U^{\tilde{b}}$ and staus $U^{\tilde{\tau}}$.

There are formulae analogous to those above for the loop corrections to the $H_{1,2,3}t\bar{t}$ vertices, which would be relevant for CP-violation measurements in $e^-e^+ \to \nu\bar{\nu}t\bar{t}$ [33], for example.

Analogous exchanges of binos and winos give finite loop-induced corrections to the $H_{1,2,3}\tau^+\tau^-$ coupling, which have a similar structure:

$$h_\tau \;=\; \frac{\sqrt{2}m_\tau}{v\cos\beta}\,\frac{1}{1+(\Delta h_\tau/h_\tau)\tan\beta}\,, \tag{2.10}$$

where

$$(\Delta h_\tau/h_\tau) \;=\; -\frac{\alpha_{\rm em}\,\mu^* M_2^*}{4\pi\, s_W^2}\Bigg[\,I(m^2_{\tilde{\nu}_\tau},|M_2|^2,|\mu|^2)\;+\;\frac{1}{2}\,|U^{\tilde{\tau}}_{L1}|^2\, I(m^2_{\tilde{\tau}_1},|M_2|^2,|\mu|^2)$$

$$
\begin{aligned}
&+\frac{1}{2}\,|U^{\tilde{\tau}}_{L2}|^2\,I(m^2_{\tilde{\tau}_2},|M_2|^2,|\mu|^2)\Big]\;+\;\frac{\alpha_{\rm em}\,\mu^* M_1^*}{4\pi\,c_W^2}\Big[I(m^2_{\tilde{\tau}_1},m^2_{\tilde{\tau}_2},|M_1|^2)\\
&+\frac{1}{2}\,|U^{\tilde{\tau}}_{L1}|^2\,I(m^2_{\tilde{\tau}_1},|M_1|^2,|\mu|^2)\;+\;\frac{1}{2}\,|U^{\tilde{\tau}}_{L2}|^2\,I(m^2_{\tilde{\tau}_2},|M_1|^2,|\mu|^2)\\
&-|U^{\tilde{\tau}}_{R1}|^2\,I(m^2_{\tilde{\tau}_1},|M_1|^2,|\mu|^2)\;-\;|U^{\tilde{\tau}}_{R2}|^2\,I(m^2_{\tilde{\tau}_2},|M_1|^2,|\mu|^2)\Big]\,. \qquad (2.11)
\end{aligned}
$$

The threshold corrections modify the couplings of the neutral Higgs bosons to the scalar and pseudoscalar fermion bilinears as follows [20]:

$$
\begin{aligned}
g^S_{H_i\bar{f}f} &= \frac{O_{\phi_1 i}}{\cos\beta}\,\Re{\rm e}\left(\frac{1}{1+\kappa_f\tan\beta}\right)\;+\;\frac{O_{\phi_2 i}}{\cos\beta}\,\Re{\rm e}\left(\frac{\kappa_f}{1+\kappa_f\tan\beta}\right)\\
&\quad+O_{ai}\,\Im{\rm m}\left(\frac{\kappa_f\,(\tan^2\beta+1)}{1+\kappa_f\tan\beta}\right),\\
g^P_{H_i\bar{f}f} &= \frac{O_{\phi_1 i}}{\cos\beta}\,\Im{\rm m}\left(\frac{\kappa_f\,\tan\beta}{1+\kappa_f\tan\beta}\right)\;-\;\frac{O_{\phi_2 i}}{\cos\beta}\,\Im{\rm m}\left(\frac{\kappa_f}{1+\kappa_f\tan\beta}\right)\\
&\quad-O_{ai}\,\Re{\rm e}\left(\frac{\tan\beta-\kappa_f}{1+\kappa_f\tan\beta}\right), \qquad (2.12)
\end{aligned}
$$

where $f=b$ and τ^- and

$$
\kappa_b \;=\; \frac{(\Delta h_b/h_b)}{1+(\delta h_b/h_b)}\,, \qquad \kappa_\tau \;=\; (\Delta h_\tau/h_\tau)\,. \qquad (2.13)
$$

There are similar formulae for the $H_{1,2,3}\mu^+\mu^-$ vertices that would be relevant for $\mu^+\mu^-$ colliders. The analogous corrections to the $H_{1,2,3}e^+e^-$ vertices may be neglected.

Additional contributions to Higgs-boson vertices may arise from absorptive effects due to the opening of third-generation sfermion pair production channels. However, if the $H_{1,2,3}$-boson masses are well below the kinematic threshold of such production channels, these absorptive effects are small and can be neglected. Finally, we remind the reader that detailed analytic expressions for the effective Higgs-boson couplings to the photon, the gluon, the $W^\pm$ bosons and SUSY particles are given in [34].

3 Tau Pair Production at the LHC

To further elucidate the formalism presented in Section 2, we now discuss in more detail the production, mixing and decay of Higgs bosons into polarized $\tau^+\tau^-$ pairs at the LHC. We will study individually the three most significant production channels for Higgs bosons in the MSSM at the LHC: (i) $b\bar{b}$ fusion, (ii) gg fusion and (iii) W^+W^- fusion.

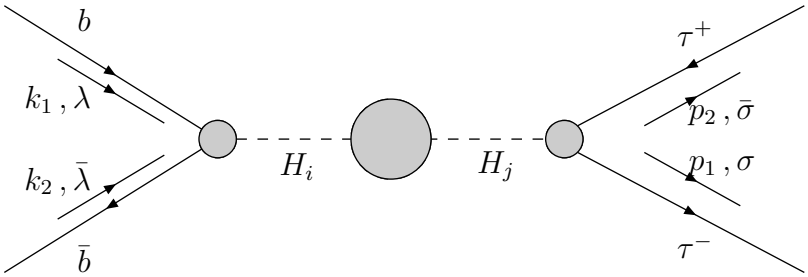

Figure 1: *Mechanisms contributing to the process $b\bar{b} \to H \to \tau^+\tau^-$, including off-diagonal absorptive parts in the Higgs-boson propagator matrix.*

3.1 $b\bar{b}$ Fusion

At large $\tan\beta$, an important mechanism for producing neutral Higgs bosons at the LHC is $b\bar{b}$ fusion [37, 38, 39, 31]. Figure 1 illustrates how the matrix element $\mathcal{M}^{b\bar{b}}$ for $b\bar{b} \to \tau^+\tau^-$ receives contributions from the s-channel exchanges of the neutral Higgs bosons. The loop-corrected propagator matrix and vertices calculated in the previous section are indicated by shaded circles. The matrix element can be written as

$$\begin{aligned}\mathcal{M}^{b\bar{b}} &= -\frac{g^2 m_b m_\tau}{4M_W^2 \hat{s}} \sum_{i,j=1,2,3} \sum_{\alpha,\beta=\pm} \Big\{ (g^S_{H_i\bar{b}b} + i\alpha g^P_{H_i\bar{b}b})\, \bar{v}(k_2,\bar{\lambda}) P_\alpha u(k_1,\lambda)\, D_{ij}(\hat{s}) \\ &\qquad \times (g^S_{H_j\tau^+\tau^-} + i\beta g^P_{H_j\tau^+\tau^-})\, \bar{u}(p_1,\sigma) P_\beta v(p_2,\bar{\sigma}) \Big\}, \end{aligned} \tag{3.1}$$

where $P_\alpha = (1+\alpha\gamma_5)/2$. We denote the helicities of τ^- and τ^+ by σ and $\bar{\sigma}$ and those of the b and $\bar{b}$ by λ and $\bar{\lambda}$, respectively, with $\sigma, \lambda = +$ and $-$ standing for right- and left-handed particles. The four-momenta of the τ^- and τ^+ are p_1 and p_2, respectively, those of the b and $\bar{b}$ are k_1 and k_2, respectively, and $\hat{s}$ is the centre-of-mass energy squared of the $\bar{b}b$ pair that fuses into a Higgs boson: $\hat{s} = (k_1+k_2)^2 = (p_1+p_2)^2$.

An important element of our formalism is the consideration of the 'full' 3×3 Higgs-boson propagator matrix $D(\hat{s})$ in (3.1) [3]. This is given by

$$D(\hat{s}) = \hat{s} \begin{pmatrix} \hat{s} - M_{H_1}^2 + i\Im\mathrm{m}\widehat{\Pi}_{11}(\hat{s}) & i\Im\mathrm{m}\widehat{\Pi}_{12}(\hat{s}) & i\Im\mathrm{m}\widehat{\Pi}_{13}(\hat{s}) \\ i\Im\mathrm{m}\widehat{\Pi}_{21}(\hat{s}) & \hat{s} - M_{H_2}^2 + i\Im\mathrm{m}\widehat{\Pi}_{22}(\hat{s}) & i\Im\mathrm{m}\widehat{\Pi}_{22}(\hat{s}) \\ i\Im\mathrm{m}\widehat{\Pi}_{31}(\hat{s}) & i\Im\mathrm{m}\widehat{\Pi}_{32}(\hat{s}) & \hat{s} - M_{H_3}^2 + i\Im\mathrm{m}\widehat{\Pi}_{33}(\hat{s}) \end{pmatrix}^{-1}. \tag{3.2}$$

[3] Strictly speaking, the complete propagator matrix $D(\hat{s})$ is a 4×4-dimensional matrix spanned by the basis (H_1, H_2, H_3, G^0) [27]. However, to a good approximation, we may neglect the small off-resonant self-energy transitions of the Higgs bosons $H_{1,2,3}$ to the neutral would-be Goldstone boson G^0.

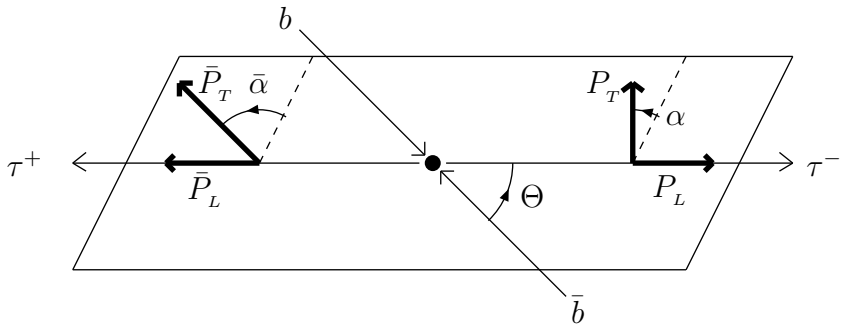

Figure 2: *The $\tau^+\tau^-$ production plane with definitions of the scattering angle Θ. The transverse polarization vectors P_T and $\bar{P}_T$ have azimuthal angles α and $\bar{\alpha}$, respectively, with respect to the event plane.*

In the above, the absorptive parts of the Higgs self-energies $\Im\mathrm{m}\widehat{\Pi}_{ij}(\hat{s})$ are given in Section 2 and $M_{H_{1,2,3}}$ are the one-loop Higgs-boson pole masses, where higher-order absorptive effects on $M_{H_{1,2,3}}$ have been ignored [15]. In the same context, the off-shell dispersive parts of the Higgs-boson self-energies in the Higgs-boson propagator matrix $D(\hat{s})$ have also been neglected, since these are formally higher-order effects and very small in the relevant Higgs-boson resonant region. Finally, we include in (3.1) the finite loop-induced corrections to the couplings of Higgs bosons to b quarks, $g^{S,P}_{H_i\bar{b}b}$, and τ leptons, $g^{S,P}_{H_j\tau^+\tau^-}$, due to the exchanges of gauginos and Higgsinos, as has been discussed in Section 2.

In the centre-of-mass coordinate system for the $b\bar{b}$ pair, the helicity amplitudes are given by

$$\mathcal{M}^{b\bar{b}}(\sigma\bar{\sigma};\lambda\bar{\lambda}) \;=\; -\frac{g^2 m_b m_\tau}{4M_W^2}\,\langle\sigma;\lambda\rangle_b \delta_{\sigma\bar{\sigma}}\delta_{\lambda\bar{\lambda}}\,, \tag{3.3}$$

where

$$\langle\sigma;\lambda\rangle_b \;\equiv\; \sum_{i,j=1,2,3} (\lambda\beta_b\, g^S_{H_i\bar{b}b} + i g^P_{H_i\bar{b}b})\, D_{ij}(\hat{s})\, (\sigma\beta_\tau\, g^S_{H_j\tau^+\tau^-} - i g^P_{H_j\tau^+\tau^-})\,, \tag{3.4}$$

with $\beta_f = \sqrt{1-4m_f^2/\hat{s}}$. Note that the cross sections for general (longitudinal or transverse) $\tau^\pm$ polarizations can be computed from the helicity amplitudes by a suitable rotation [40] from the helicity basis to a general spin basis.

The τ-polarization weighted squared matrix elements are given by

$$\overline{\left|\mathcal{M}^{b\bar{b}}\right|^2} \;=\; \frac{1}{12}\sum_{\lambda=\pm}\left(\sum_{\sigma\sigma'\bar{\sigma}\bar{\sigma}'}\mathcal{M}^{b\bar{b}}_{\sigma\bar{\sigma}}\mathcal{M}^{b\bar{b}*}_{\sigma'\bar{\sigma}'}\bar{\rho}_{\bar{\sigma}'\bar{\sigma}}\rho_{\sigma'\sigma}\right) \;=\; \frac{1}{12}\sum_{\lambda=\pm}\mathrm{Tr}\left[\mathcal{M}^{b\bar{b}}\bar{\rho}^T\mathcal{M}^{b\bar{b}\dagger}\rho\right]\,, \tag{3.5}$$

where ρ and $\bar{\rho}$ are 2×2 polarization density matrices for the τ^- and τ^+, respectively:

$$\rho \;=\; \frac{1}{2}\begin{pmatrix} 1+P_L & P_T\,\mathrm{e}^{-i\alpha} \\ P_T\,\mathrm{e}^{i\alpha} & 1-P_L \end{pmatrix}\,, \qquad \bar{\rho} \;=\; \frac{1}{2}\begin{pmatrix} 1+\bar{P}_L & -\bar{P}_T\,\mathrm{e}^{i\bar{\alpha}} \\ -\bar{P}_T\,\mathrm{e}^{-i\bar{\alpha}} & 1-\bar{P}_L \end{pmatrix}\,. \tag{3.6}$$

Evaluating the trace in (3.5) yields

$$\overline{\left|\mathcal{M}^{b\bar{b}}\right|^2} \;=\; \frac{1}{12}\left(\frac{g^2 m_b m_\tau}{4M_W^2}\right)^2 \Big\{ C_1^b(1+P_L\bar{P}_L) + C_2^b(P_L+\bar{P}_L) \\ + P_T\bar{P}_T\left[C_3^b\cos(\alpha-\bar{\alpha}) + C_4^b\sin(\alpha-\bar{\alpha})\right]\Big\}. \qquad (3.7)$$

The $\tau^+\tau^-$ production plane is depicted schematically in Fig. 2, where the transverse polarization angles α and $\bar{\alpha}$ are also defined.

The coefficients $C_n^b (n = 1-4)$ in (3.7) are defined in terms of the helicity amplitudes by

$$C_1^b \;\equiv\; \frac{1}{4}\sum_{\lambda=\pm}\left(|\langle +;\lambda\rangle_b|^2 + |\langle -;\lambda\rangle_b|^2\right), \qquad C_2^b \;\equiv\; \frac{1}{4}\sum_{\lambda=\pm}\left(|\langle +;\lambda\rangle_b|^2 - |\langle -;\lambda\rangle_b|^2\right), \\ C_3^b \;\equiv\; -\frac{1}{2}\sum_{\lambda=\pm}\Re\mathrm{e}\left(\langle +;\lambda\rangle_b\langle -;\lambda\rangle_b^*\right), \qquad C_4^b \;\equiv\; \frac{1}{2}\sum_{\lambda=\pm}\Im\mathrm{m}\left(\langle +;\lambda\rangle_b\langle -;\lambda\rangle_b^*\right). \qquad (3.8)$$

Under CP and CP$\widetilde{\mathrm{T}}$ [4] transformations, the helicity amplitudes transform as follows:

$$\langle\sigma;\lambda\rangle_b \overset{\mathrm{CP}}{\leftrightarrow} +\langle -\sigma;-\lambda\rangle_b, \qquad \langle\sigma;\lambda\rangle_b \overset{\mathrm{CP\widetilde{T}}}{\leftrightarrow} +\langle -\sigma;-\lambda\rangle_b^*. \qquad (3.9)$$

Hence, the CP and CP$\widetilde{\mathrm{T}}$ parities of the coefficients C_n^b defined in (3.8) are given by

$$C_1^b[++], \qquad C_2^b[--], \qquad C_3^b[++], \qquad C_4^b[-+], \qquad (3.10)$$

where the first and second symbols in the square brackets are the CP and CP$\widetilde{\mathrm{T}}$ parities, respectively. Consequently, the coefficients C_2^b and C_4^b signify genuine phenomena of CP violation, whereas C_1^b and C_3^b are CP-conserving. Here, we should remark that a non-zero value for the CP$\widetilde{\mathrm{T}}$-odd coefficient C_2^b can only be induced by non-vanishing absorptive effects. In our case, such effects mainly originate from the absorptive parts of the Higgs-boson self-energies.

Finally, for our phenomenological discussion in Section 4, we define the parton-level cross sections

$$\hat{\sigma}_i(b\bar{b}\to H\to\tau^+\tau^-) \;\equiv\; \frac{\beta_\tau}{192\pi\hat{s}}\left(\frac{g^2 m_b m_\tau}{4M_W^2}\right)^2 C_i^b, \qquad (3.11)$$

where the intermediate state H collectively denotes all the $H_i \to H_j$ resonant transitions with $i, j = 1, 2, 3$.

[4] We define $\widetilde{\mathrm{T}}$ as the naive T-reversal transformation, under which the spins and 3-momenta of the asymptotic states reverse sign, without interchanging initial to final states. In addition, under the operation of $\widetilde{\mathrm{T}}$, the matrix element gets complex conjugated.

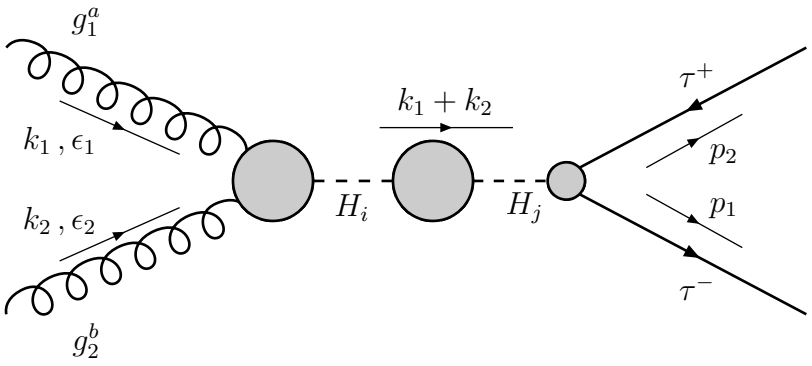

Figure 3: *Mechanisms contributing to the process $gg \to H \to \tau^+\tau^-$ via the three neutral Higgs bosons $H_{1,2,3}$.*

3.2 gg Fusion

The matrix element $\mathcal{M}^{gg}$ for the process $gg \to H \to \tau^+\tau^-$, depicted in Fig. 3, can be written as

$$\mathcal{M}^{gg} = \frac{g\alpha_s m_\tau \delta^{ab}}{8\pi v M_W} \times \sum_{i,j=1,2,3}^{3} \sum_{\alpha=\pm} G_{H_i}(k_1,\epsilon_1;k_2,\epsilon_2)\, D_{ij}(\hat{s})\, (g^S_{H_j\tau^+\tau^-} + i\alpha g^P_{H_j\tau^+\tau^-})\, \bar{u}(p_1,\sigma) P_\alpha v(p_2,\bar{\sigma})\,. \quad (3.12)$$

In the above, a and b are indices of the SU(3) generators in the adjoint representation and $k_{1,2}$ and $\epsilon_{1,2}$ are the four-momenta and wave vectors of the two gluons, respectively. Again, we denote the helicities of τ^- and τ^+ by σ and $\bar{\sigma}$ with $\sigma = +$ and $-$ standing for right- and left-handed particles. The four-momenta of τ^- and τ^+ are p_1 and p_2, respectively, and $\hat{s} = (k_1+k_2)^2 = (p_1+p_2)^2$. The Higgs-boson propagator matrix $D(\hat{s})$ was given in (3.2) and the loop-induced couplings of the Higgs bosons H_i to two gluons are given by

$$G_{H_i}(k_1,\epsilon_1;k_2,\epsilon_2) = i\, S_i^g(\sqrt{\hat{s}}) \left(\epsilon_1\cdot\epsilon_2 - \frac{2}{\hat{s}}\, k_1\cdot\epsilon_2 k_2\cdot\epsilon_1\right) - i\, P_i^g(\sqrt{\hat{s}})\, \frac{2}{\hat{s}}\, \varepsilon_{\mu\nu\rho\sigma}\epsilon_1^\mu\epsilon_2^\nu k_1^\rho k_2^\sigma\,, \quad (3.13)$$

with $\varepsilon_{0123} = 1$. For the loop functions S_i^g and P_i^g, we follow the definitions of [34].

In the two-gluon centre-of-mass coordinate system with $\mathbf{k}_1$ along the positive z direction and $\mathbf{k}_2$ along the negative z direction, the wave vectors of two photons are given by

$$\epsilon_1^\mu(\lambda_1) = \frac{1}{\sqrt{2}}\left(0,-\lambda_1,-i,0\right), \qquad \epsilon_2^\mu(\lambda_2) = \frac{1}{\sqrt{2}}\left(0,-\lambda_2,i,0\right), \quad (3.14)$$

where $\lambda = +1$ and -1 denote the right and left gluon helicities, respectively. The helicity amplitudes are given by

$$\mathcal{M}^{gg}(\sigma\bar{\sigma};\lambda_1\lambda_2) \;=\; \frac{g\alpha_s m_\tau\sqrt{\hat{s}}\delta^{ab}}{8\pi v M_W}\langle\sigma;\lambda_1\rangle_g\delta_{\sigma\bar{\sigma}}\delta_{\lambda_1\lambda_2}\,, \tag{3.15}$$

where the amplitude $\langle\sigma;\lambda\rangle_g$ is defined as

$$\langle\sigma;\lambda\rangle_g \equiv \sum_{i,j=1,2,3}\left[S_i^g(\sqrt{\hat{s}}) + i\lambda P_i^g(\sqrt{\hat{s}})\right] D_{ij}(\hat{s})\,\left(\sigma\beta_\tau g^S_{H_j\tau^+\tau^-} - i g^P_{H_j\tau^+\tau^-}\right). \tag{3.16}$$

We note that the amplitude (3.15) has the same structure as the amplitude (3.3) for $b\bar{b}\to\tau^+\tau^-$, except for the overall constant. We obtain from the helicity amplitudes the polarization-weighted squared matrix elements given by

$$\begin{aligned}\overline{|\mathcal{M}^{gg}|^2} \;=\; \frac{1}{32}\left(\frac{g\alpha_s m_\tau\sqrt{\hat{s}}}{8\pi v M_W}\right)^2\Big\{&C_1^g(1+P_L\bar{P}_L) + C_2^g(P_L+\bar{P}_L)\\ &+P_T\bar{P}_T\left[C_3^g\cos(\alpha-\bar{\alpha}) + C_4^g\sin(\alpha-\bar{\alpha})\right]\Big\}, \end{aligned}\tag{3.17}$$

where the coefficients C_n^g are obtained by replacing $\langle\sigma;\lambda\rangle_b \to \langle\sigma;\lambda\rangle_g$ and interpreting λ as the gluon helicity in (3.8).

Under the CP and CP$\widetilde{\rm T}$ transformations, the helicity amplitudes transform as follows:

$$\langle\sigma;\lambda\rangle_g \overset{\rm CP}{\leftrightarrow} -\langle-\sigma;-\lambda\rangle_g\,, \qquad \langle\sigma;\lambda\rangle_g \overset{\rm CP\widetilde{T}}{\leftrightarrow} -\langle-\sigma;-\lambda\rangle_g^*\,, \tag{3.18}$$

where the CP and CP$\widetilde{\rm T}$ parities of the coefficients C_i^g are the same as those of the C_i^b. Finally, we define the parton-level cross sections as:

$$\hat{\sigma}_i(gg\to H\to\tau^+\tau^-) \;\equiv\; \frac{\beta_\tau}{512\pi\hat{s}}\left(\frac{g\alpha_s m_\tau\sqrt{\hat{s}}}{8\pi v M_W}\right)^2 C_i^g\,. \tag{3.19}$$

Note that the CP- and CP$\widetilde{\rm T}$-odd cross section $\hat{\sigma}_2$ receives contributions from the absorptive parts of the $H_{1,2,3}gg$ vertices and Higgs-boson self-energies as well.

3.3 W^+W^- Fusion

The last important mechanism for the production of the MSSM neutral Higgs bosons at the LHC is W^+W^- fusion [41, 42, 43, 44]. The matrix element $\mathcal{M}^{WW}$ for this process, $W^-(k_1)W^+(k_2)\to H\to\tau^-(p_1)\tau^+(p_2)$ with $\hat{s}=(k_1+k_2)^2$, is given by

$$\mathcal{M}^{WW} \;=\; \frac{g^2 m_\tau}{2\hat{s}}\sum_{i,j=1}^{3}\sum_{\alpha=\pm} g_{H_iVV}\,\epsilon_1\cdot\epsilon_2\,D_{ij}(\hat{s})\,(g^S_{H_j\tau^+\tau^-} + i\alpha g^P_{H_j\tau^+\tau^-})\,\bar{u}(p_1,\sigma)P_\alpha v(p_2,\bar{\sigma})\,, \tag{3.20}$$

where ϵ_1 and ϵ_2 are the polarization vectors of two vector bosons and g_{H_iVV} denotes the coupling of the Higgs boson H_i with a pair of gauge bosons, as defined through the interaction Lagrangian

$$\mathcal{L}_{HVV} \;=\; gM_W\left(W^+_\mu W^{-\mu} + \frac{1}{2c_W^2}Z_\mu Z^\mu\right)\sum_{i=1}^{3} g_{H_iVV}H_i\,. \tag{3.21}$$

In the W^+W^- centre-of-mass coordinate system with $\mathbf{k}_1$ along the positive z direction and $\mathbf{k}_2$ along the negative z direction, the polarization vectors of two vector bosons are given by

$$\begin{aligned}
\epsilon_1^\mu(\lambda_1=\pm1) \;&=\; \frac{1}{\sqrt{2}}\Big(0,\mp1,-i,0\Big)\,, \qquad & \epsilon_1^\mu(\lambda_1=0) \;&=\; \frac{1}{\sqrt{k_1^2}}\Big(|\mathbf{k}_1|,0,0,k_1^0\Big)\,,\\
\epsilon_2^\mu(\lambda_2=\pm1) \;&=\; \frac{1}{\sqrt{2}}\Big(0,\mp1,i,0\Big)\,, \qquad & \epsilon_2^\mu(\lambda_2=0) \;&=\; \frac{1}{\sqrt{k_2^2}}\Big(|\mathbf{k}_2|,0,0,-k_2^0\Big)\,,
\end{aligned} \tag{3.22}$$

where the polarization vectors are normalized by $\epsilon_i(\lambda)\cdot\epsilon_i^*(\lambda') = -\delta_{\lambda\lambda'}$, and $\lambda=\pm1$ and $\lambda=0$ denote the transverse (right and left helicities) and longitudinal polarizations, respectively. In this frame, the helicity amplitude is given by

$$\mathcal{M}^{WW}(\sigma\bar\sigma;\lambda_1\lambda_2) \;=\; \frac{g^2m_\tau}{2\sqrt{\hat s}}\langle\sigma;\lambda_1\rangle_W\delta_{\sigma\bar\sigma}\delta_{\lambda_1\lambda_2}\,, \tag{3.23}$$

where the amplitude $\langle\sigma;\lambda\rangle_W$ is defined by

$$\langle\sigma;\lambda\rangle_W \;\equiv\; \sum_{i,j=1,2,3}\omega(\lambda)\,g_{H_iVV}\,D_{ij}(\hat s)\,(\sigma\beta_\tau\,g^S_{H_j\tau^+\tau^-} - ig^P_{H_j\tau^+\tau^-})\,, \tag{3.24}$$

with

$$\omega(\pm)=1 \quad\text{and}\quad \omega(0) = -k_1\cdot k_2/\sqrt{k_1^2k_2^2}\,. \tag{3.25}$$

The factor $\omega(0)$ becomes $1-\hat s/2M_W^2$ for on-shell vector bosons and dominates the amplitude for $\hat s \gg M_W$.

One can then obtain the following averaged amplitude squared:

$$\begin{aligned}
\overline{|\mathcal{M}^{WW}|^2} \;=\; \frac{1}{9}\left(\frac{g^2m_\tau}{2\sqrt{\hat s}}\right)^2\Big\{&C_1^W(1+P_L\bar P_L) + C_2^W(P_L+\bar P_L)\\
&+P_T\bar P_T\left[C_3^W\cos(\alpha-\bar\alpha) + C_4^W\sin(\alpha-\bar\alpha)\right]\Big\}\,,
\end{aligned} \tag{3.26}$$

where the coefficients C_n^W can be obtained by replacing $\langle\sigma;\lambda\rangle_b \to \langle\sigma;\lambda\rangle_W$ and summing over $\lambda=\pm,0$ in (3.8). The CP and CP$\widetilde{\rm T}$ parities of the coefficients C_n^W are the same as those of C_n^b or C_n^g, and the parton-level cross sections are defined similarly as

$$\hat\sigma_i(W^+_{T,L}W^-_{T,L}\to H\to\tau^+\tau^-) \;\equiv\; \frac{\beta_\tau}{144\,\pi\hat s}\left(\frac{g^2m_\tau}{2\sqrt{\hat s}}\right)^2 C_i^W\,. \tag{3.27}$$

In kinematic situations where the longitudinal $W_L^+W_L^-$ contributions can be neglected, the average factor 1/144 should be replaced by 1/64. Finally, we note that it is straightforward to calculate ZZ-fusion processes in a similar fashion, although their cross sections are smaller approximately by a factor of 4 than W^+W^- collisions at the hadron level.

4 Numerical Examples

We now present some numerical examples of CP-violating Higgs signatures in $\tau^+\tau^-$ production at the LHC. As already mentioned, these signatures may be enhanced at large $\tan\beta$, and three-way mixing is potentially important for small charged Higgs-boson masses. Since the prospects for observing $H_{1,2,3} \to \tau^+\tau^-$ at the LHC are best for light Higgs bosons, we present in this section some numerical analyses in a specific scenario in which all the three Higgs states mix significantly.

Explicitly, we take the following parameter set:

$$\begin{aligned}
&\tan\beta = 50, \quad M_{H^\pm}^{\rm pole} = 155 \ \text{GeV}, \\
&M_{\tilde{Q}_3} = M_{\tilde{U}_3} = M_{\tilde{D}_3} = M_{\tilde{L}_3} = M_{\tilde{E}_3} = M_{\rm SUSY} = 0.5 \ \text{TeV}, \\
&|\mu| = 0.5 \ \text{TeV}, \quad |A_{t,b,\tau}| = 1 \ \text{TeV}, \quad |M_2| = |M_1| = 0.3 \ \text{TeV}, \quad |M_3| = 1 \ \text{TeV}, \\
&\Phi_\mu = 0^\circ, \quad \Phi_A = \Phi_{A_t} = \Phi_{A_b} = \Phi_{A_\tau} = 90^\circ, \quad \Phi_1 = \Phi_2 = 0^\circ,
\end{aligned} \tag{4.1}$$

and we consider two values for the phase of the gluino mass parameter M_3: $\Phi_3 = -90^\circ\,, -10^\circ$. For $\Phi_3 = -10^\circ$, `CPsuperH` yields for the masses and widths of the neutral Higgs bosons:

$$\begin{aligned}
&M_{H_1} = 120.2 \ \text{GeV}, \quad M_{H_2} = 121.4 \ \text{GeV}, \quad M_{H_3} = 124.5 \ \text{GeV}, \\
&\Gamma_{H_1} = 1.19 \ \text{GeV}, \quad \Gamma_{H_2} = 3.42 \ \text{GeV}, \quad \Gamma_{H_3} = 3.20 \ \text{GeV},
\end{aligned} \tag{4.2}$$

and for $\Phi_3 = -90^\circ$:

$$\begin{aligned}
&M_{H_1} = 118.4 \ \text{GeV}, \quad M_{H_2} = 119.0 \ \text{GeV}, \quad M_{H_3} = 122.5 \ \text{GeV}, \\
&\Gamma_{H_1} = 3.91 \ \text{GeV}, \quad \Gamma_{H_2} = 6.02 \ \text{GeV}, \quad \Gamma_{H_3} = 6.34 \ \text{GeV},
\end{aligned} \tag{4.3}$$

respectively.

In Figs. 4 and 5, we show the parton-level cross sections $\hat{\sigma}_i(b\bar{b} \to H \to \tau^+\tau^-)$, $\hat{\sigma}_i(gg \to H \to \tau^+\tau^-)$ and $\hat{\sigma}_i(WW \to H \to \tau^+\tau^-)$ defined in (3.11), (3.19) and (3.27), respectively, as functions of the $\tau^+\tau^-$ invariant mass $\sqrt{\hat{s}}$. The solid lines are for $\Phi_3 = -90^\circ$ and the dashed (red) ones for $\Phi_3 = -10^\circ$. We recall that non-vanishing of $\hat{\sigma}_2$ and $\hat{\sigma}_4$

are direct signals of CP violation in longitudinally and transversally polarized $\tau^+\tau^-$ pairs, respectively.

The parton-level cross sections $\hat{\sigma}_i(WW \to \tau^+\tau^-)$ have been computed by neglecting the contribution of the longitudinally-polarized $W^\pm$, i.e., setting $\omega(0) = 0$. For the MSSM scenario defined in (4.1), this is a plausible approximation for Higgs-boson masses below the WW threshold. Possible uncertainties that such a treatment may introduce largely cancel when we consider ratios of the cross sections $\hat{\sigma}_i(WW \to \tau^+\tau^-)$, such as the CP asymmetries to be defined later in this section.

In Fig. 4, we observe that the cross section $\hat{\sigma}_2$, which quantifies CP violation in the production of longitudinally polarized τ-lepton pairs at the parton level, is comparable to the spin-averaged cross section $\hat{\sigma}_1$ in WW and gg collisions. This implies that CP violation can be very large in these channels. Instead, in $b\bar{b}$ fusion, the ratio $\hat{\sigma}_2/\hat{\sigma}_1$ is always less than 1%, so CP-violating effects in the production of longitudinally polarized τ leptons are unobservably small in this case.

The smallness of $\hat{\sigma}_2$ in $b\bar{b}$ fusion is a result of an intriguing interplay between unitarity and CPT invariance [27]. In detail, the CP-violating cross section $\hat{\sigma}_2$ may be calculated by

$$\hat{\sigma}_2(b\bar{b} \to H \to \tau^+\tau^-) \;=\; \frac{1}{4}\left[\,\hat{\sigma}(b\bar{b} \to H \to \tau_R^+\tau_R^-) \;-\; \hat{\sigma}(b\bar{b} \to H \to \tau_L^+\tau_L^-)\,\right], \tag{4.4}$$

where $\hat{\sigma}$ denotes the usual subprocess cross section. For the scenario under study, unitarity cuts of $b\bar{b}$ pairs dominate the absorptive part of the Higgs-boson self-energies. Employing this fact and the optical theorem, we obtain

$$\begin{aligned}\sum_{\lambda=L,R} \hat{\sigma}_2(b_\lambda\bar{b}_\lambda \to H \to \tau^+\tau^-) \;&=\; C_{\rm PS}\Big(\,\Im{\rm m}\,\mathcal{T}(\tau_R^+\tau_R^- \to H \to \tau_R^+\tau_R^-) \\ &\quad - \Im{\rm m}\,\mathcal{T}(\tau_L^+\tau_L^- \to H \to \tau_L^+\tau_L^-)\,\Big) \;+\; \mathcal{O}\Big[\hat{\sigma}_2'\,B(H_{1,2,3} \to \tau^+\tau^-)\Big]\,,\end{aligned} \tag{4.5}$$

where $C_{\rm PS}$ is a phase-space correction factor and $\mathcal{T}(\tau_{L,R}^+\tau_{L,R}^- \to H \to \tau_{L,R}^+\tau_{L,R}^-)$ denote the usual matrix elements. In (4.5), $\hat{\sigma}_2'$ is the CP-violating cross-section $\hat{\sigma}_2$ calculated by omitting the off-diagonal absorptive parts in the Higgs-boson propagator matrix $D(\hat{s})$. The size of $\hat{\sigma}_2'$ is smaller at least by a factor 10 than the spin-averaged cross-section $\hat{\sigma}_1$. On the other hand, CPT invariance imposes the constraint

$$\mathcal{T}(\tau_R^+\tau_R^- \to H \to \tau_R^+\tau_R^-) \;=\; \mathcal{T}(\tau_L^+\tau_L^- \to H \to \tau_L^+\tau_L^-)\,. \tag{4.6}$$

With the aid of (4.6), it is not difficult to see using (4.5) that the CP-violating cross section $\hat{\sigma}_2(b\bar{b} \to H \to \tau^+\tau^-)$ vanishes up to CP-violating terms suppressed by extra factors of order $B(H_{1,2,3} \to \tau^+\tau^-)$.

Our numerical estimates presented in Fig. 5 show that the CP-violating transverse-polarization cross section $\hat{\sigma}_4$ may be quite sizeable for all production channels. However, $\hat{\sigma}_4$ generically exhibits an alternating sign for $b\bar{b}$ and gg collisions, and CP violation becomes very small when we integrate over the whole Higgs-boson resonance region. Moreover, the transverse $\tau^{\pm}$ polarizations will be difficult to measure at the LHC because of the experimental conditions, notably the large boosts of the $\tau^{\pm}$. On the other hand, analogous asymmetries might be observable in $\bar{t}t$ production and/or in $\tau^+\tau^-$ production at a $\mu^+\mu^-$ collider.

The Higgs production channels via $b\bar{b}$ and gg fusion processes can be separated from the W^+W^- fusion channel by applying a number of kinematic cuts [45] including the imposition of a veto on any hadronic activity between jets [46, 47]. Therefore, we treat the contributions from $b\bar{b}$ and gg collisions to the physical Higgs-exchange process $pp \to H \to \tau^+\tau^- X$ separately from those coming from WW fusion. More explicitly, the physical $\tau^+\tau^-$ cross section can be computed by integrating the parton-level cross sections with the distribution of b quarks, gluons and W-bosons in the proton,

$$\begin{aligned} \tau\,\frac{d\sigma_{\rm tot}}{d\tau}\left(pp\,(b\bar{b},gg)\;\to\;\tau^+\tau^- X\right) \;&=\; 4\,\hat{\sigma}_1(b\bar{b}\to H\to\tau^+\tau^-)\;\tau\,\frac{d\mathcal{L}^{bb}}{d\tau} \\ &\quad +4\;K\,\hat{\sigma}_1(gg\to H\to\tau^+\tau^-)\;\tau\,\frac{d\mathcal{L}^{gg}}{d\tau}\,, \qquad (4.7) \end{aligned}$$

$$\tau\,\frac{d\sigma_{\rm tot}}{d\tau}\left(pp\,(W^+W^-)\;\to\;\tau^+\tau^- X\right) \;=\; 4\,\hat{\sigma}_1(W^+W^-\to H\to\tau^+\tau^-)\;\tau\,\frac{d\mathcal{L}^{WW}}{d\tau}\,, \quad (4.8)$$

where τ is the Drell–Yan variable $\tau = \hat{s}/s$ and s is the invariant squared centre-of-mass energy of the LHC. In (4.7), we use the value $K = 1 + \frac{\alpha_s(\hat{s})}{\pi}\,(\pi^2 + 11/2)$, ignoring the small difference between the $K-$factors for CP-even and CP-odd Higgs states. The effective luminosities for $b\bar{b}$ and gg collisions, $\mathcal{L}^{bb}$ and $\mathcal{L}^{gg}$, may be determined by

$$\begin{aligned} \tau\frac{d\mathcal{L}^{bb}}{d\tau} \;&=\; \int_\tau^1 dx\,\left[\,\frac{\tau}{x}\,b(x,Q)\,\bar{b}\left(\frac{\tau}{x},Q\right)\;+\;(b\leftrightarrow\bar{b})\right]\,, \\ \tau\frac{d\mathcal{L}^{gg}}{d\tau} \;&=\; \int_\tau^1 dx\,\frac{\tau}{x}\,g(x,Q)\,g\left(\frac{\tau}{x},Q\right)\,, \qquad (4.9) \end{aligned}$$

where $b(x,Q)$, $\bar{b}(x,Q)$ and $g(x,Q)$ are the b, $\bar{b}$ and gluon distribution functions in the proton and Q is the factorization scale. In our numerical analysis, we use the leading-order CTEQ6L [48] parton distribution functions for $b(x,Q)$ and $\bar{b}(x,Q)$, and the CTEQ6M parton distribution function for $g(x,Q)$. We choose the factorization scale $Q = \sqrt{\hat{s}}/4$ for the b-quark fusion process as suggested and confirmed in [38].

Correspondingly, in (4.8), the effective luminosities for the transverse and longitudinal W-bosons, denoted as $W^{\pm}_{T,L}$, can be computed in terms of effective densities $F^p_{W^{\pm}_{T,L}}(x,Q)$ in

the colliding protons, which are in turn calculated in terms of the quark parton distribution functions $q(x,Q)$ in the proton:[5]

$$\begin{aligned}
\tau\,\frac{d\mathcal{L}^{W_PW_P}}{d\tau} &= \int_\tau^1 dx\,\left[\frac{\tau}{x}\,F^p_{W_P^+}(x,Q)\,F^p_{W_P^-}\!\left(\frac{\tau}{x},Q\right)\;+\;(W_P^+\leftrightarrow W_P^-)\right],\\
F^p_{W_P^+}(x,Q) &= \sum_{q=u,\bar d,c,\bar s}\int_x^1\frac{dy}{y}\;q(y,Q)\,F^q_{W_P^+}(x/y,Q)\,,
\end{aligned}\tag{4.10}$$

where the transverse ($P=T$) and longitudinal ($P=L$) effective densities $F^q_{W^+_{T,L}}$ in the quark q are given by [42, 43]

$$\begin{aligned}
F^q_{W_T^+}(x,Q) &= \frac{\alpha_{\rm em}}{8\pi\,s_W^2}\;\ln\!\left(\frac{Q^2}{M_W^2}\right)\;\frac{1+(1-x)^2}{x}\,,\\
F^q_{W_L^+}(x,Q) &= \frac{\alpha_{\rm em}}{4\pi\,s_W^2}\;\frac{1-x}{x}\,.
\end{aligned}\tag{4.11}$$

Note that the summation over quark flavours q in the expression for $F^p_{W^-_{T,L}}(x,Q)$ includes $q=\bar u,d,\bar c,s$. Moreover, we take $Q=\sqrt{\hat s}$ in our numerical estimates.

To analyze the signatures of CP violation in the production of longitudinally polarized τ-leptons, we first define the physical observables

$$\sigma_{RR}\;=\;\sigma(pp\;\to\;H\;\to\;\tau_R^+\tau_R^-X)\,,\qquad \sigma_{LL}\;=\;\sigma(pp\;\to\;H\;\to\;\tau_L^+\tau_L^-X)\,.\tag{4.12}$$

Evidently, the total cross section for Higgs production and decay into $\tau^+\tau^-$ pairs is given in terms of σ_{RR} and σ_{LL} by

$$\sigma_{\rm tot}(pp\;\to\;H\;\to\;\tau^+\tau^-X)\;=\;\sigma_{RR}\;+\;\sigma_{LL}\;.\tag{4.13}$$

Although the initial state pp is not symmetric under CP, it can, however, be shown that, up to negligible higher-order CP-violating electroweak effects, the effective luminosities for gg, $b\bar b$ and W^+W^- densities will be practically the same for pp and $\bar p\bar p$ collisions. Therefore, the difference of cross sections

$$\Delta\sigma_{\rm CP}\;=\;\sigma_{RR}\;-\;\sigma_{LL}\tag{4.14}$$

is a measure of genuine CP violation at the LHC. In analogy with (4.7) and (4.8), the CP-violating cross section $\Delta\sigma_{\rm CP}$ can be computed by

$$\begin{aligned}
\tau\,\frac{d\Delta\sigma_{\rm CP}}{d\tau}\Big(pp\,(b\bar b,gg)\;\to\;\tau^+\tau^-X\Big) &= 4\,\hat\sigma_2\,(b\bar b\to H\to\tau^+\tau^-)\;\tau\,\frac{d\mathcal{L}^{bb}}{d\tau}\\
&\quad+\,4\,K\,\hat\sigma_2\,(gg\to H\to\tau^+\tau^-)\;\tau\,\frac{d\mathcal{L}^{gg}}{d\tau}\,,
\end{aligned}\tag{4.15}$$

$$\tau\,\frac{d\Delta\sigma_{\rm CP}}{d\tau}\Big(pp\,(W^+W^-)\;\to\;\tau^+\tau^-X\Big)\;=\;4\,\hat\sigma_2(W^+W^-\to H\to\tau^+\tau^-)\;\tau\,\frac{d\mathcal{L}^{WW}}{d\tau}\,.\tag{4.16}$$

[5]Here we consider identical polarizations for the $W^\pm$ bosons in the W^+W^- fusion process.

To gauge the sizes of the signatures of CP violation at the LHC, we define the following two CP asymmetries:

$$a_{\rm CP}(\tau) \;\equiv\; \frac{\tau\,\dfrac{d\Delta\sigma_{\rm CP}}{d\tau}}{\tau\,\dfrac{d\sigma_{\rm tot}}{d\tau}}\;, \qquad\qquad \mathcal{A}_{\rm CP} \;\equiv\; \frac{\Delta\sigma_{\rm CP}}{\sigma_{\rm tot}}\;, \tag{4.17}$$

pertinent to the hadron-level processes $pp\,(b\bar{b}, gg, WW) \;\to\; H \;\to\; \tau^+\tau^- X$.

We plot in Fig. 6 the differential cross sections $\tau\,\frac{d\sigma_{\rm tot}}{d\tau}$ and $\tau\,\frac{d\Delta\sigma_{\rm CP}}{d\tau}$ as functions of $\sqrt{\hat{s}}$. The upper two frames are for the process $b\bar{b} \to \tau^+\tau^-$, the frames in the middle for $gg \to \tau^+\tau^-$, and the lower ones for $W^+W^- \to \tau^+\tau^-$. We observe that the the main production mechanism is $b\bar{b}$ fusion, which gives a cross section about five times larger than that due to gluon fusion for the scenario under consideration. However, as has been mentioned above, the W^+W^--fusion production mechanism, albeit much smaller, can be experimentally distinguished from that due to $b\bar{b}$ and gg collisions. Therefore, in Fig. 7 we display the CP asymmetry $a_{\rm CP}$ defined in (4.17) separately for the $b\bar{b} + gg$ and W^+W^- subprocesses. We note that the large CP asymmetry in gg subprocess is diluted by the dominant cross section via $b\bar{b}$ fusion[6].

Although CP violation in the WW and gg production channels may be sizeable, it is difficult to measure the differential CP asymmetry $a_{\rm CP}$ at the LHC because of the low energy resolution of the reconstructed $\tau^+\tau^-$ invariant mass. This last fact also limits our ability to reconstruct with sufficient accuracy the line shape of the decaying coupled Higgs-boson system at the LHC. This is unfortunate since one would miss the very interesting feature shown in Fig. 6 that, unlike the case of a single resonance, the locations of the various maxima in the resonant line shapes described by $\tau\,\frac{d\sigma_{\rm tot}}{d\tau}$ crucially depend on the production and decay channels of the coupled Higgs-boson system. Therefore, the extra analyzing power of e^+e^- and $\mu^+\mu^-$ colliders would be highly valuable for unravelling the existence of a strongly-mixed Higgs-boson system and studying in more detail its dynamical properties.

Motivated by the large differential CP asymmetry in the W^+W^--fusion process, we perform a numerical analysis of the total CP asymmetry for the reaction $pp(WW) \to H \to \tau^+\tau^-$, integrated over the Higgs resonance peaks. We present in Figs. 8, 9 and 10 the predicted values for the cross-section $\sigma_{\rm tot}(pp(WW) \to H \to \tau^+\tau^- X)$ and its associated total integrated CP asymmetry $\mathcal{A}_{\rm CP}^{WW}$ defined in (4.17) as functions of $\Phi_A = \Phi_{A_t} = \Phi_{A_b} = \Phi_{A_\tau}$, for $\Phi_3 = -10^\circ$, -70°, and -90°, respectively. In the upper two frames of the figures,

[6]Specifically, the total CP asymmetry in the gg subprocess is $\mathcal{A}_{\rm CP}^{gg} = -8.4\,(-6.2)\,\%$, for $\Phi_3 = -90^\circ\,(-10^\circ)$. However, after the inclusion of $b\bar{b}$ collisions, the combined CP asymmetry $\mathcal{A}_{\rm CP}^{b\bar{b}+gg}$ reduces to $-1.4\,(-1.0)\,\%$.

we display the dependence of the Higgs-boson masses and their decay widths on the CP-violating phase Φ_A, where the solid, dashed and dotted lines refer to the H_1, H_2 and H_3 bosons, respectively. In our numerical analysis, we fix the remaining parameters of the MSSM as in (4.1). Unlike in Figs. 8, 9, and 10, we present in Fig. 11 numerical estimates by fixing the value of Φ_A to -90°, but varying the CP-violating phase Φ_3. For the scenario under study, all three Higgs bosons mix among themselves significantly, giving rise to level crossings as the CP-odd phases vary. These effects of level crossing lead to a non-trivial behaviour in Γ_{H_i}, which is between 1 GeV and 10 GeV [7], and in $\mathcal{A}_{\rm CP}^{WW}$. We find that the total cross section is between 0.1 pb and 0.7 pb and is comparable to the corresponding SM cross section 0.3 pb for $M_{H_{\rm SM}} = 120$ GeV [45]. We observe that the CP asymmetry $\mathcal{A}_{\rm CP}^{WW}$ is large for a wide range of CP phases and can even be as large as 80% for $\Phi_3 = -70^\circ$. Even for small CP-violating phases, $\Phi_3 = -10^\circ$ and $(180^\circ - |\Phi_A|) < 20^\circ$, the CP asymmetry can be $\sim 50\%$, as shown in Fig. 8. Again, we note that possible uncertainties in the calculation of the cross sections largely cancel in the CP asymmetry $\mathcal{A}_{\rm CP}$.

Finally, we comment briefly on the possible impact of low-energy constraints on the CP asymmetries, especially those arising from the non-observation of the electron and neutron EDMs and the absence of the Higgs-mediated B-meson decay $B_{s,d} \to \mu\mu$ at the Tevatron [49]. The EDM constraints may be considerably relaxed if we consider scenarios with the first two generations of squarks heavier than about 3 TeV, and if we allow some degree of cancellations [6] between the one- and higher-loop EDM contributions [50]. For the scenarios under study, we have estimated that the required degree of cancellation is always smaller than 80%, where 100% corresponds to complete cancellation. Therefore, a full implementation of EDM constraints will not alter the results of the present analysis in a significant way. On the other hand, the lack of observation of $B_{s,d} \to \mu\mu$ at the Tevatron [49] imposes further constraints on the parameters of the CP-violating MSSM. However, the derived constraints are highly flavour-dependent and can be dramatically relaxed for certain choices of the soft SUSY-breaking mass spectrum that enable unitarity cancellations in the flavour space. For a detailed study, see [9].

[7] In Fig. 11, the widths of the H_1 and H_2 become larger than 10 GeV when $\Phi_3 > 100^\circ$ or $\Phi_3 < -140^\circ$, where M_{H_1} decreases very rapidly and H_1 decouples from the $H_2 - H_3$ mixing system.

5 Conclusions and Prospects

We have presented the general formalism for analyzing CP-violating phenomena in the production, mixing and decay of a coupled system of multiple CP-violating neutral Higgs bosons. Our formalism, which is developed from [27], can be applied to models with an extended CP-violating Higgs sector, including the highly predictive framework of the MSSM with radiative Higgs-sector CP violation. An important element of the formalism is the consideration of the full s-dependent 3×3 Higgs-boson propagator matrix, where the gauge-mediated contributions to self-energies have been calculated in the framework of the Pinch Technique [30, 35].

As an application of our formalism, we have studied in detail the production of CP-violating MSSM $H_{1,2,3}$ bosons via $\bar{b}b$, gg and W^+W^- collisions and their subsequent decays into $\tau^+\tau^-$ pairs at the LHC. In addition to the Higgs self-energy effects, we have also given explicitly the relevant formulae in the MSSM with loop-induced CP violation in the production and decay vertices. We have considered specific MSSM scenarios that predict three nearly degenerate, strongly-mixed Higgs bosons with $M_{H_{1,2,3}} \sim 120$ GeV. Such scenarios naturally occur in a general CP-violating MSSM when $\tan\beta$ is larger than 30 and the charged Higgs boson is lighter than about 160 GeV.

We have analyzed CP asymmetries in both longitudinally- and transversely-polarized $\tau^+\tau^-$ pairs. CP asymmetries that make use of the transverse polarization of the τ-lepton, although being intrinsically very large in the CP-violating MSSM scenarios mentioned above, generically exhibit an alternating sign and become unobservably small after averaging over the entire Higgs-boson resonant region. Also, reconstruction of transversely polarized τ leptons appears rather difficult at the LHC. However, such CP asymmetries might ideally be tested at a $\mu^+\mu^-$ collider, where a high energy resolution can be achieved.

At the LHC, more promising are CP asymmetries based on the longitudinal τ-lepton polarization. In particular, the CP asymmetry in the production channel $W^+W^- \to H_{1,2,3} \to \tau^+\tau^-$ may well exceed the 10% level and reach values up to 80%. It is important to stress again that the WW production channel can be cleanly isolated from the gg and $b\bar{b}$ channels, mainly by vetoing any hadronic activity between jets (for details, see [45]). Hence, depending on the efficiency of longitudinal τ-lepton polarization techniques [51], the production channel $W^+W^- \to H_{1,2,3} \to \tau^+\tau^-$ may become the 'golden' channel for studying signatures of Higgs-sector CP violation at the LHC.

The formalism presented in this paper may easily be applied to other colliders as well, most notably to e^+e^-, $\gamma\gamma$ and $\mu^+\mu^-$ colliders. At e^+e^- linear colliders, Higgs bosons can copiously be produced via the Higgsstrahlung or W^+W^- fusion processes. At $\gamma\gamma$

and $\mu^+\mu^-$ colliders, the polarizations of the colliding beams may also be varied, thereby providing additional probes of Higgs-sector CP violation. The aforementioned colliders can provide cleaner experimental conditions than the LHC. Consequently, even if the CP asymmetries discussed here prove difficult to observe at the LHC, the formalism and the analysis techniques developed here to investigate Higgs-sector CP violation will be directly applicable to such future colliders as well.

Acknowledgements

We thank Jeff Forshaw for discussions. The work of JSL and AP is supported in part by the PPARC research grant PPA/G/O/2000/00461.

References

[1] For reviews, see, H.P. Nilles, Phys. Rep. **110** (1984) 1; H. Haber and G. Kane, Phys. Rep. **117** (1985) 75; J.F. Gunion, H.E. Haber, G.L. Kane and S. Dawson, *The Higgs Hunter's Guide*, (Addison-Wesley, Reading, MA, 1990).

[2] S. Y. Choi, J. Kalinowski, G. Moortgat-Pick and P. M. Zerwas, Eur. Phys. J. C **22** (2001) 563; S. Y. Choi, A. Djouadi, M. Guchait, J. Kalinowski, H. S. Song and P. M. Zerwas, Eur. Phys. J. C **14** (2000) 535; A. Bartl, S. Hesselbach, K. Hidaka, T. Kernreiter and W. Porod, Phys. Lett. B **573** (2003) 153; A. Bartl, H. Fraas, O. Kittel and W. Majerotto, Phys. Rev. D **69** (2004) 035007.

[3] For a review, see D. J. H. Chung, L. L. Everett, G. L. Kane, S. F. King, J. Lykken and L. T. Wang, hep-ph/0312378.

[4] A. Pilaftsis, Phys. Rev. D **58** (1998) 096010; Phys. Lett. B **435** (1998) 88.

[5] J. Ellis, S. Ferrara and D.V. Nanopoulos, Phys. Lett. B **114** (1982) 231; W. Buchmüller and D. Wyler, Phys. Lett. B **121** (1983) 321; J. Polchinski and M. Wise, Phys. Lett. B **125** (1983) 393; F. del Aguila, M. Gavela, J. Grifols and A. Mendez, Phys. Lett. B **126** (1983) 71; M. Dugan, B. Grinstein and L. Hall, Nucl. Phys. B **255** (1985) 413; R. Garisto and J.D. Wells, Phys. Rev. D **55** (1997) 1611.

[6] T. Ibrahim and P. Nath, Phys. Rev. D **58** (1998) 111301; Phys. Rev. D **61** (2000) 093004; M. Brhlik, L. Everett, G.L. Kane and J. Lykken, Phys. Rev. Lett. **83** (1999) 2124; Phys. Rev. D **62** (2000) 035005; S. Pokorski, J. Rosiek and C.A. Savoy, Nucl. Phys. B **570** (2000) 81; E. Accomando, R. Arnowitt and B. Dutta, Phys. Rev. D **61** (2000) 115003; A. Bartl, T. Gajdosik, W. Porod, P. Stockinger and H. Stremnitzer, Phys. Rev. D **60** (1999) 073003; T. Falk, K.A. Olive, M. Pospelov and R. Roiban, Nucl. Phys. B **60** (1999) 3; S.A. Abel, S. Khalil and O. Lebedev, Nucl. Phys. B **606** (2001) 151.

[7] For discussions on Higgs-mediated EDMs in the MSSM with explicit CP violation, see D. Chang, W.-Y. Keung and A. Pilaftsis, Phys. Rev. Lett. **82** (1999) 900; A. Pilaftsis, Nucl. Phys. B **644** (2002) 263; D. A. Demir, O. Lebedev, K. A. Olive, M. Pospelov and A. Ritz, Nucl. Phys. B **680** (2004) 339.

[8] For recent studies in the CP-violating MSSM, see P.H. Chankowski and Lucja Slawianowska, Phys. Rev. D **63** (2001) 054012; C.S. Huang, W. Liao, Q.-S. Yuan and S.-H. Zhu, Phys. Rev. D **63** (2001) 114021; D. A. Demir and K. A. Olive, Phys.

Rev. D **65** (2002) 034007; M. Boz and N. K. Pak, Phys. Lett. B **531** (2002) 119; A. J. Buras, P. H. Chankowski, J. Rosiek and L. Slawianowska, Nucl. Phys. B **659** (2003) 3; T. Ibrahim and P. Nath, Phys. Rev. D **67** (2003) 016005; Phys. Rev. D **67** (2003) 095003.

[9] For the general resummed form of the effective Lagrangian for Higgs-mediated FCNC interactions, see A. Dedes and A. Pilaftsis, Phys. Rev. D **67** (2003) 015012.

[10] A. Pilaftsis and C.E.M. Wagner, Nucl. Phys. B **553** (1999) 3.

[11] D.A. Demir, Phys. Rev. D **60** (1999) 055006.

[12] S.Y. Choi, M. Drees and J.S. Lee, Phys. Lett. B **481** (2000) 57.

[13] M. Carena, J. Ellis, A. Pilaftsis and C.E.M. Wagner, Nucl. Phys. B **586** (2000) 92.

[14] T. Ibrahim and P. Nath, Phys. Rev. D **63** (2001) 035009; Phys. Rev. D **66** (2002) 015005; T. Ibrahim, Phys. Rev. D **64** (2001) 035009; S. W. Ham, S. K. Oh, E. J. Yoo, C. M. Kim and D. Son, Phys. Rev. D **68** (2003) 055003.

[15] M. Carena, J. Ellis, A. Pilaftsis and C.E.M. Wagner, Nucl. Phys. B **625** (2002) 345.

[16] G.L. Kane and L.-T. Wang, Phys. Lett. B **488** (2000) 383.

[17] S. Heinemeyer, Eur. Phys. J. C **22** (2001) 521.

[18] S.Y. Choi and J.S. Lee, Phys. Rev. D **61** (2000) 015003; S.Y. Choi, K. Hagiwara and J.S. Lee, Phys. Rev. D **64** (2001) 032004; S. Y. Choi, M. Drees, J. S. Lee and J. Song, Eur. Phys. J. C **25** (2002) 307.

[19] M. Carena, J. Ellis, A. Pilaftsis and C.E.M. Wagner, Phys. Lett. B **495** (2000) 155.

[20] M. Carena, J. Ellis, S. Mrenna, A. Pilaftsis and C.E.M. Wagner, Nucl. Phys. B **659** (2003) 145.

[21] A. Dedes and S. Moretti, Phys. Rev. Lett. **84** (2000) 22; Nucl. Phys. B **576** (2000) 29; S.Y. Choi and J.S. Lee, Phys. Rev. D **61** (2000) 115002; S.Y. Choi, K. Hagiwara and J.S. Lee, Phys. Lett. B **529** (2002) 212; A. Arhrib, D. K. Ghosh and O.C. Kong, Phys. Lett. B **537** (2002) 217; E. Christova, H. Eberl, W. Majerotto and S. Kraml, Nucl. Phys. B **639** (2002) 263; JHEP **0212** (2002) 021; W. Khater and P. Osland, Nucl. Phys. B **661** (2003) 209.

[22] B.E. Cox, J.R. Forshaw, J.S. Lee, J.W. Monk and A. Pilaftsis, Phys. Rev. D **68** (2003) 075004; A.G. Akeroyd, Phys. Rev. D **68** (2003) 077701.

[23] V.A. Khoze, A.D. Martin and M.G. Ryskin, hep-ph/0401078.

[24] B. Grzadkowski, J. F. Gunion and J. Kalinowski, Phys. Rev. D **60** (1999) 075011; A.G. Akeroyd and A. Arhrib, Phys. Rev. D **64** (2001) 095018.

[25] S. Y. Choi and J. S. Lee, Phys. Rev. D **62** (2000) 036005; E. Asakawa, S. Y. Choi, K. Hagiwara and J.S. Lee, Phys. Rev. D **62** (2000) 115005; J. S. Lee, hep-ph/0106327; S. Y. Choi, B. C. Chung, P. Ko and J. S. Lee, Phys. Rev. D **66** (2002) 016009; R. M. Godbole, S. D. Rindani and R. K. Singh, Phys. Rev. D **67** (2003) 095009.

[26] D. Atwood and A. Soni, Phys. Rev. D **52** (1995) 6271; B. Grzadkowski and J.F. Gunion, Phys. Lett. B **350** (1995) 218; A. Pilaftsis, Phys. Rev. Lett. **77** (1996) 4996; S.Y. Choi and J.S. Lee, Phys. Rev. D **61** (2000) 111702; E. Asakawa, S.Y. Choi and J.S. Lee, Phys. Rev. D **63** (2001) 015012; S.Y. Choi, M. Drees, B. Gaissmaier and J.S. Lee, Phys. Rev. D **64** (2001) 095009; M.S. Berger, Phys. Rev. Lett. **87** (2001) 131801; C. Blochinger *et al.*, hep-ph/0202199.

[27] A. Pilaftsis, Nucl. Phys. B **504** (1997) 61.

[28] J. Papavassiliou and A. Pilaftsis, Phys. Rev. Lett. **75** (1995) 3060; Phys. Rev. D **53** (1996) 2128; Phys. Rev. D **54** (1996) 5315.

[29] For studies of the PT beyond the one-loop level, see, D. Binosi and J. Papavassiliou, Phys. Rev. D **66** (2002) 111901; Phys. Rev. D **66** (2002) 025024; J. Phys. G **30** (2004) 203; D. Binosi, hep-ph/0401182.

[30] J.M. Cornwall, Phys. Rev. D **26** (1982) 1453; J. M. Cornwall and J. Papavassiliou, Phys. Rev. D **40** (1989) 3474; J. Papavassiliou, Phys. Rev. D **41** (1990) 3179; Phys. Rev. D **50** (1994) 5958; G. Degrassi and A. Sirlin, Phys. Rev. D **46** (1992) 3104. S. Hashimoto, J. Kodaira, Y. Yasui, and K. Sasaki, Phys. Rev. D **50** (1994) 7066; N.J. Watson, Phys. Lett. B **349** (1995) 155.

[31] F. Borzumati, J. S. Lee and W. Y. Song, hep-ph/0401024.

[32] S. Y. Choi, J. Kalinowski, J. S. Lee, M. M. Muhlleitner, M. Spira and P. M. Zerwas, hep-ph/0404119.

[33] A. Pilaftsis and M. Nowakowski, Int. J. Mod. Phys. A **9** (1994) 1097; B. Grzadkowski, Phys. Lett. B **338** (1994) 71.

[34] J. S. Lee, A. Pilaftsis, M. Carena, S. Y. Choi, M. Drees, J. R. Ellis and C. E. M. Wagner, Comput. Phys. Commun. **156** (2004) 283 [arXiv:hep-ph/0307377].

[35] J. Papavassiliou and A. Pilaftsis, Phys. Rev. Lett. **80** (1998) 2785; Phys. Rev. D **58** (1998) 053002.

[36] J. Guasch, W. Hollik and S. Penaranda, Phys. Lett. B **515** (2001) 367; M. Carena, S. Mrenna and C. E. M. Wagner, Phys. Rev. D **60** (1999) 075010; Phys. Rev. D **62** (2000) 055008; T. Ibrahim and P. Nath, Phys. Rev. D **69** (2004) 075001.

[37] D. A. Dicus and S. Willenbrock, Phys. Rev. D **39** (1989) 751; D. Dicus, T. Stelzer, Z. Sullivan and S. Willenbrock, Phys. Rev. D **59** (1999) 094016; C. Balazs, H. J. He and C. P. Yuan, Phys. Rev. D **60** (1999) 114001.

[38] J. Campbell, R. K. Ellis, F. Maltoni and S. Willenbrock, Phys. Rev. D **67** (2003) 095002; F. Maltoni, Z. Sullivan and S. Willenbrock, Phys. Rev. D **67** (2003) 093005; E. Boos and T. Plehn, hep-ph/0304034; R. V. Harlander and W. B. Kilgore, Phys. Rev. D **68** (2003) 013001; S. Dittmaier, M. Kramer and M. Spira, hep-ph/0309204; S. Dawson, C. B. Jackson, L. Reina and D. Wackeroth, hep-ph/0311067.

[39] J. j. Cao, G. p. Gao, R. J. Oakes and J. M. Yang, Phys. Rev. D **68** (2003) 075012; H. S. Hou, W. G. Ma, R. Y. Zhang, Y. B. Sun and P. Wu, JHEP **0309** (2003) 074.

[40] K. Hagiwara and D. Zeppenfeld, Nucl. Phys. B **274** (1986) 1.

[41] R. N. Cahn and S. Dawson, Phys. Lett. B **136** (1984) 196 [Erratum-ibid. B **138** (1984) 464].

[42] S. Dawson, Nucl. Phys. B **249** (1985) 42; G. L. Kane, W. W. Repko and W. B. Rolnick, Phys. Lett. B **148** (1984) 367; J. Lindfors, Phys. Lett. B **167** (1986) 471.

[43] R. M. Godbole and S. D. Rindani, Phys. Lett. B **190** (1987) 192; T. Han, G. Valencia and S. Willenbrock, Phys. Rev. Lett. **69** (1992) 3274; I. Kuss and H. Spiesberger, Phys. Rev. D **53** (1996) 6078.

[44] D. L. Rainwater, D. Zeppenfeld and K. Hagiwara, Phys. Rev. D **59** (1999) 014037; T. Plehn, D. L. Rainwater and D. Zeppenfeld, Phys. Rev. D **61** (2000) 093005.

[45] For instance, see S. Asai *et al.*, hep-ph/0402254.

[46] R. N. Cahn, S. D. Ellis, R. Kleiss and W. J. Stirling, Phys. Rev. D **35** (1987) 1626; V. D. Barger, T. Han and R. J. N. Phillips, Phys. Rev. D **37** (1988) 2005; K. Iordanidis

and D. Zeppenfeld, Phys. Rev. D **57** (1998) 3072; D. L. Rainwater and D. Zeppenfeld, Phys. Rev. D **60** (1999) 113004 [Erratum-ibid. D **61** (2000) 099901].

[47] J. M. Butterworth, B. E. Cox and J. R. Forshaw, Phys. Rev. D **65** (2002) 096014.

[48] J. Pumplin, D. R. Stump, J. Huston, H. L. Lai, P. Nadolsky and W. K. Tung, JHEP **0207** (2002) 012.

[49] D. Acosta *et al.* [CDF Collaboration], arXiv:hep-ex/0403032.

[50] See A. Pilaftsis in [7].

[51] T. Pierzchala, E. Richter-Was, Z. Was and M. Worek, Acta Phys. Polon. B **32** (2001) 1277; S. Moretti and D. P. Roy, Phys. Lett. B **545** (2002) 329.

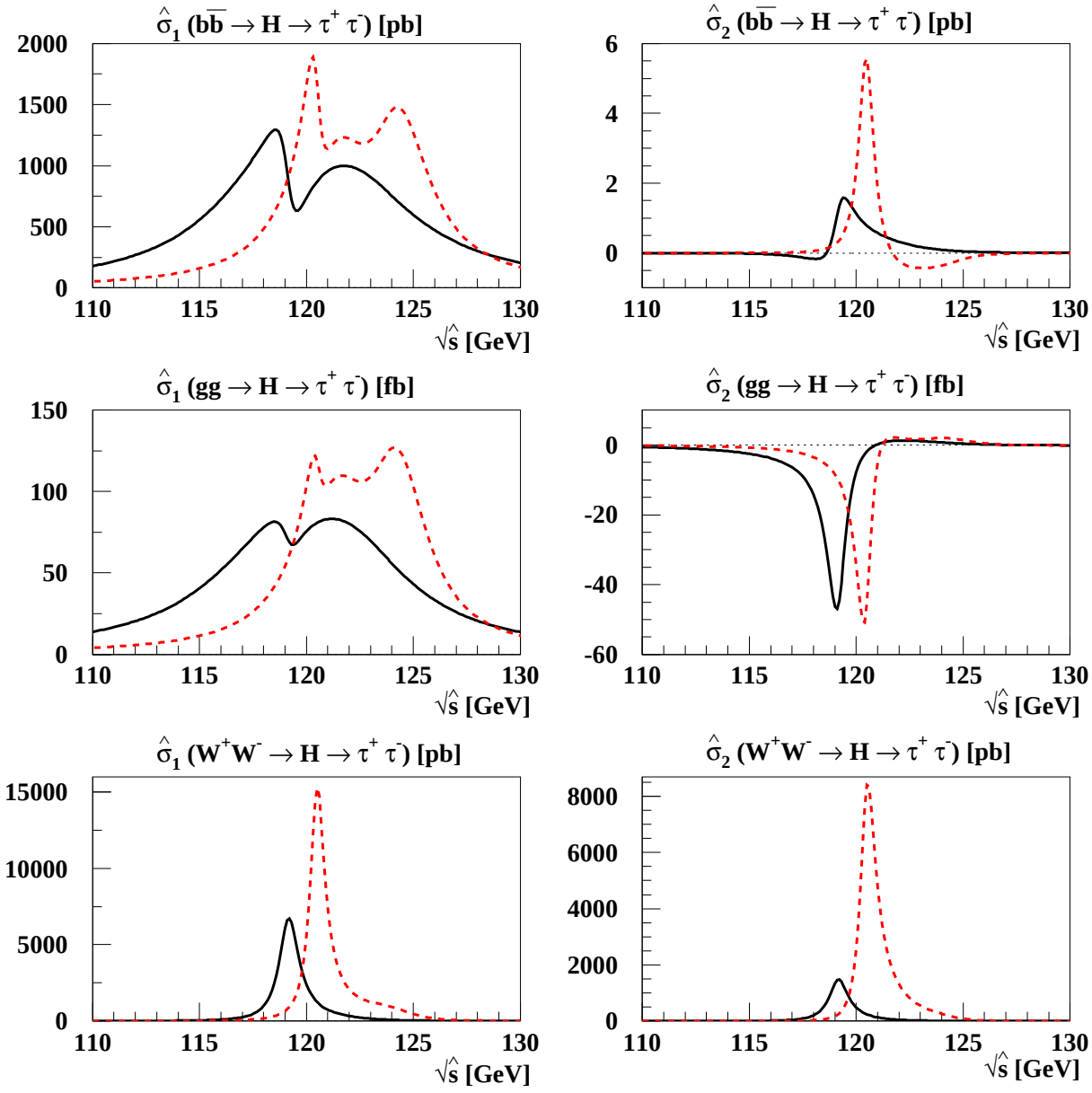

Figure 4: *The parton-level cross sections* $\hat{\sigma}_{1,2}(b\bar{b} \to H \to \tau^+\tau^-)$ *in pb,* $\hat{\sigma}_{1,2}(gg \to H \to \tau^+\tau^-)$ *in fb, and* $\hat{\sigma}_{1,2}(W^+W^- \to H \to \tau^+\tau^-)$ *in pb as functions of* $\sqrt{\hat{s}}$*. The solid lines are for the three-Higgs mixing scenario with* $\Phi_3 = -90°$ *and the dashed ones with* $\Phi_3 = -10°$*.*

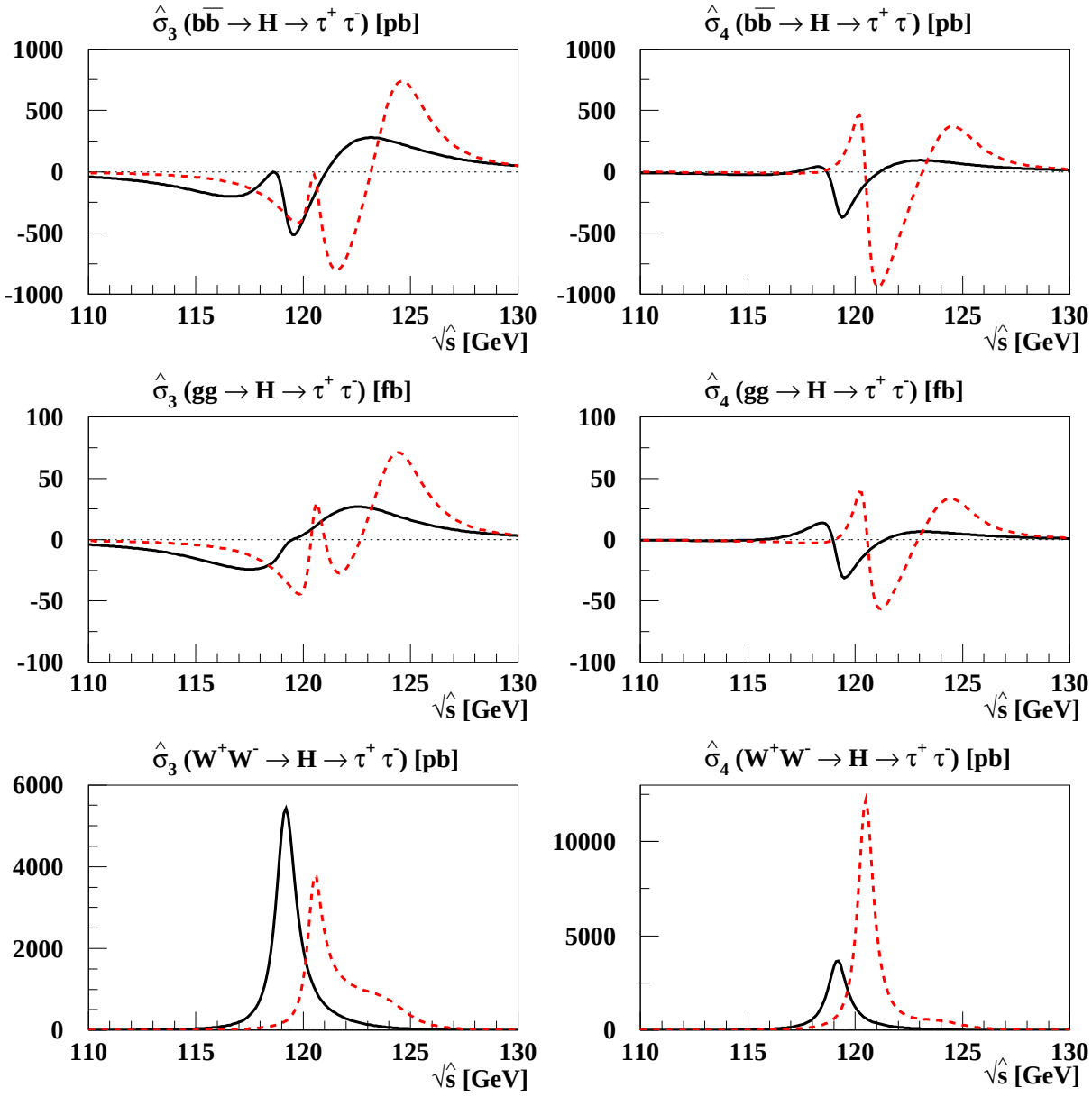

Figure 5: *The parton-level cross sections* $\hat{\sigma}_{3,4}(b\bar{b} \to H \to \tau^+\tau^-)$ *in pb,* $\hat{\sigma}_{3,4}(gg \to H \to \tau^+\tau^-)$ *in fb, and* $\hat{\sigma}_{3,4}(W^+W^- \to H \to \tau^+\tau^-)$ *in pb as functions of* $\sqrt{\hat{s}}$*. The solid lines are for the three-Higgs mixing scenario with* $\Phi_3 = -90°$ *and the dashed ones with* $\Phi_3 = -10°$*.*

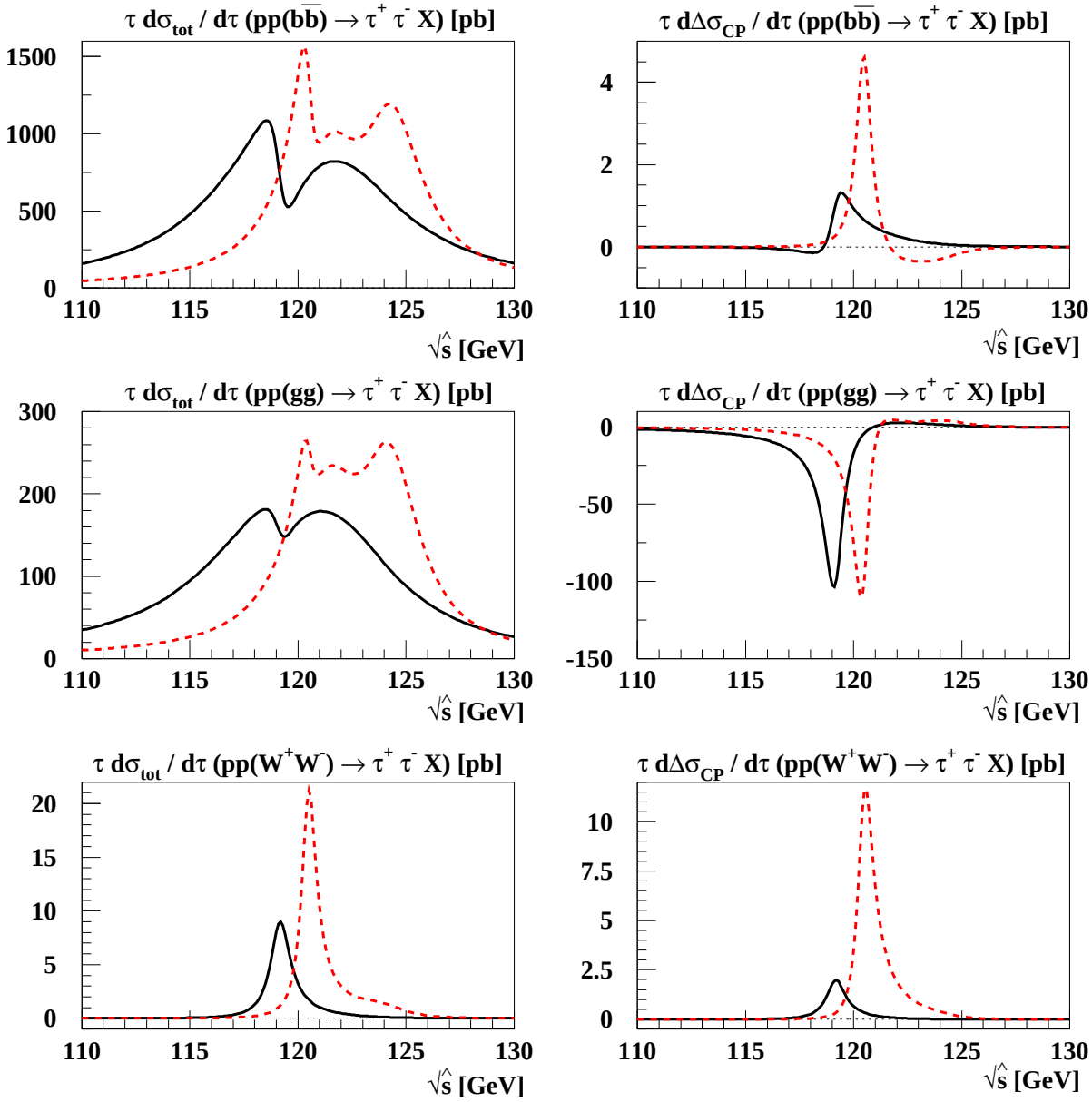

Figure 6: *The differential cross sections* $\tau \frac{d\sigma_{\rm tot}}{d\tau}$ *and* $\tau \frac{d\Delta\sigma_{\rm CP}}{d\tau}$ *as functions of* $\sqrt{\hat{s}}$. *The upper frames are for the process* $b\bar{b} \to H \to \tau^+\tau^-$, *the middle ones for* $gg \to H \to \tau^+\tau^-$ *and the lower ones for* $W^+W^- \to H \to \tau^+\tau^-$. *The solid lines are for the three-Higgs mixing scenario with* $\Phi_3 = -90^\circ$ *and the dashed ones with* $\Phi_3 = -10^\circ$.

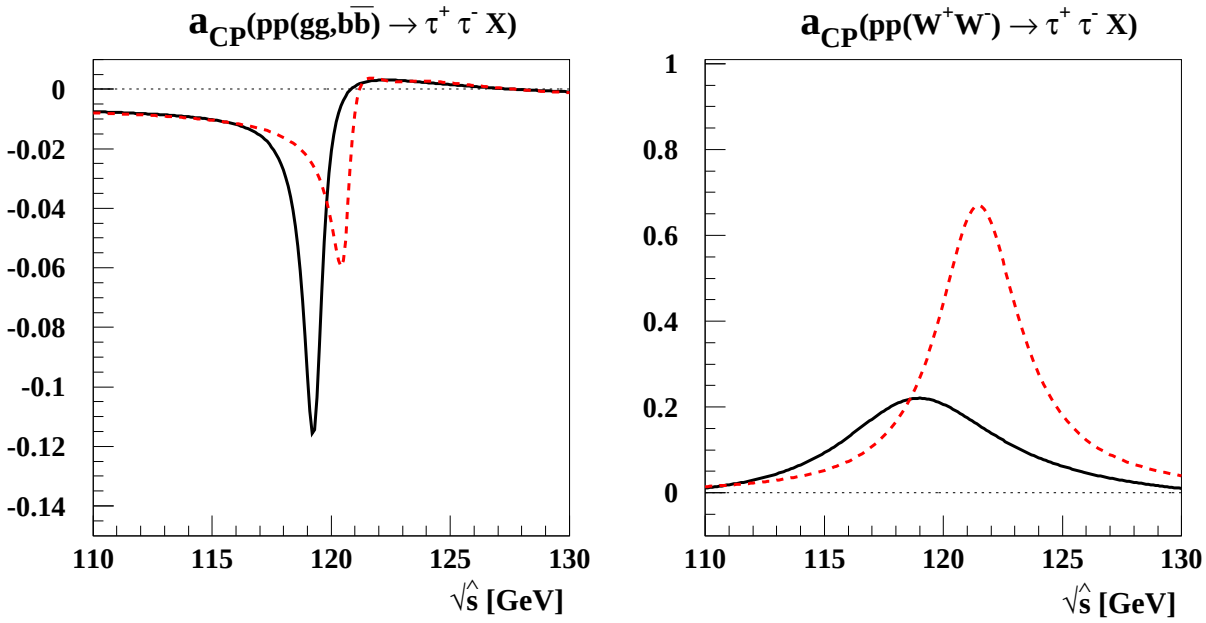

Figure 7: *Numerical estimates of differential CP asymmetries* $a_{\rm CP}$ *defined in (4.17) as functions of* $\sqrt{\hat{s}}$*. The solid line corresponds to the three-Higgs mixing scenario with* $\Phi_3 = -90^\circ$ *and the dashed one to* $\Phi_3 = -10^\circ$*.*

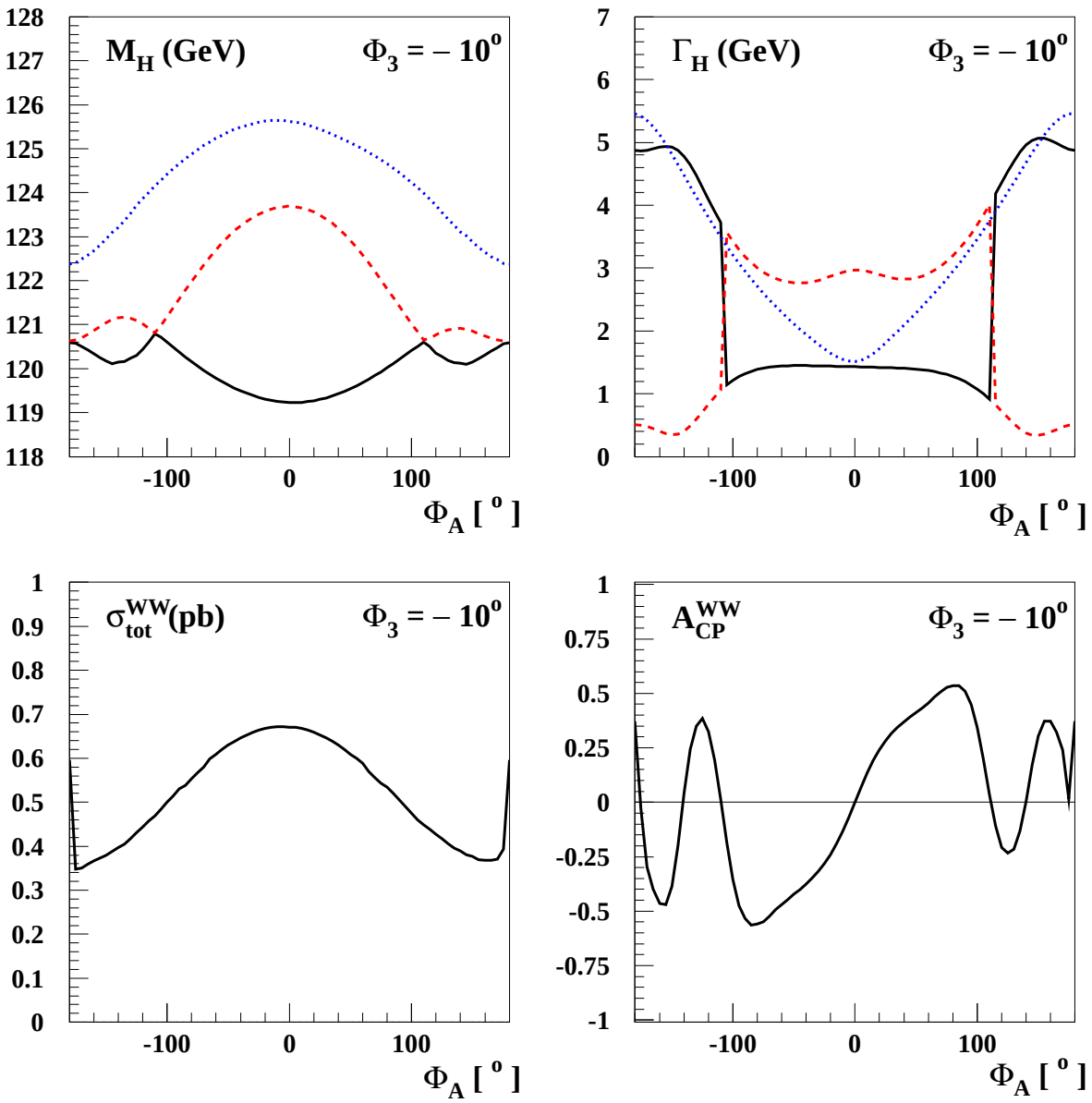

Figure 8: *Numerical estimates of Higgs-boson masses and decay widths, the cross-section* $\sigma_{\rm tot}(pp(WW) \to H \to \tau^+\tau^- X)$ *and its associated total CP asymmetry* $\mathcal{A}_{\rm CP}^{WW}$ *defined in (4.17) as functions of* $\Phi_A = \Phi_{A_t} = \Phi_{A_b} = \Phi_{A_\tau}$*, for* $\Phi_3 = -10^\circ$*. In the upper two frames, the solid, dashed and dotted lines refer to the* H_1*,* H_2 *and* H_3 *bosons, respectively.*

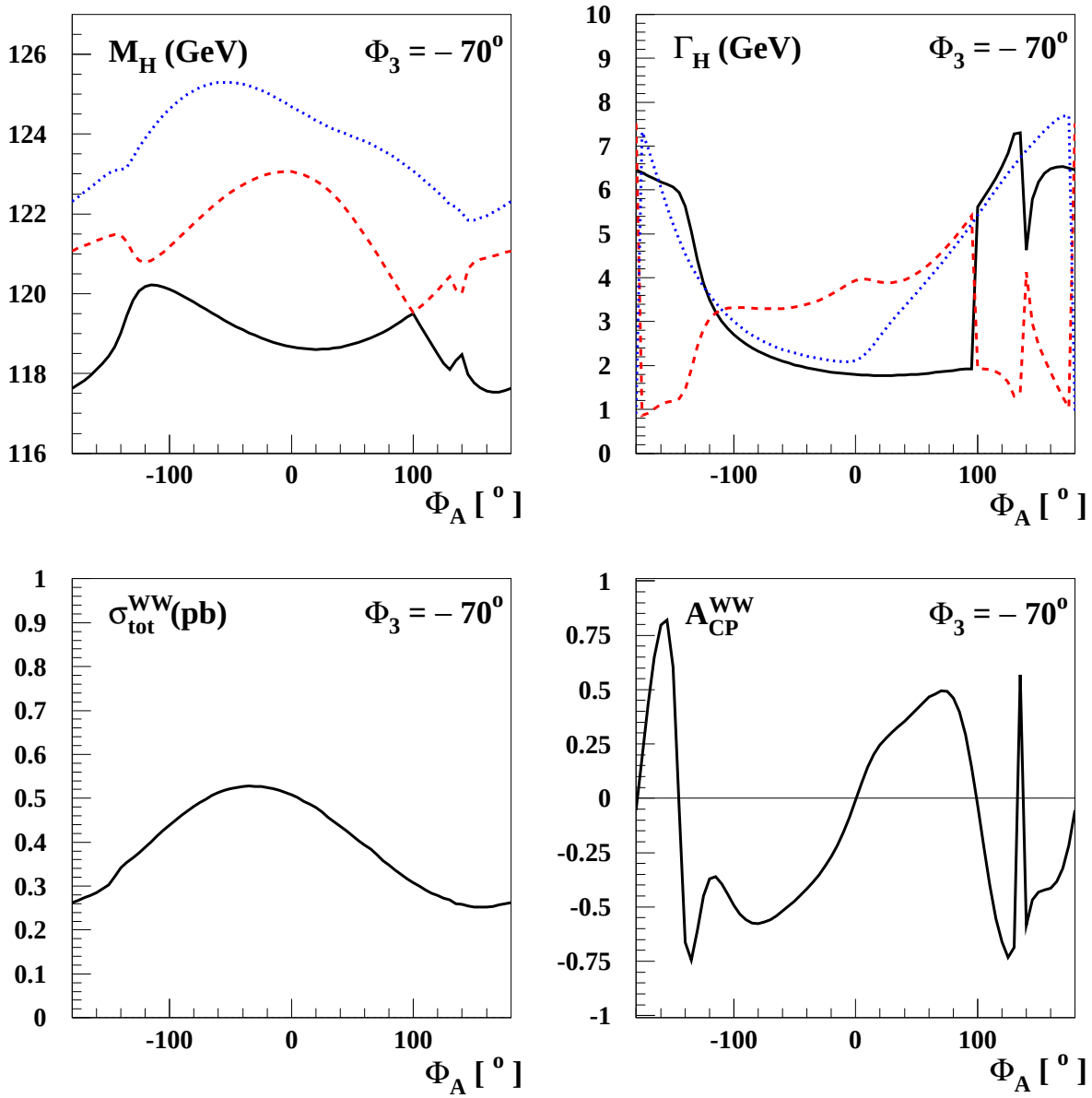

Figure 9: *The same as in Fig. 8, but for* $\Phi_3 = -70°$.

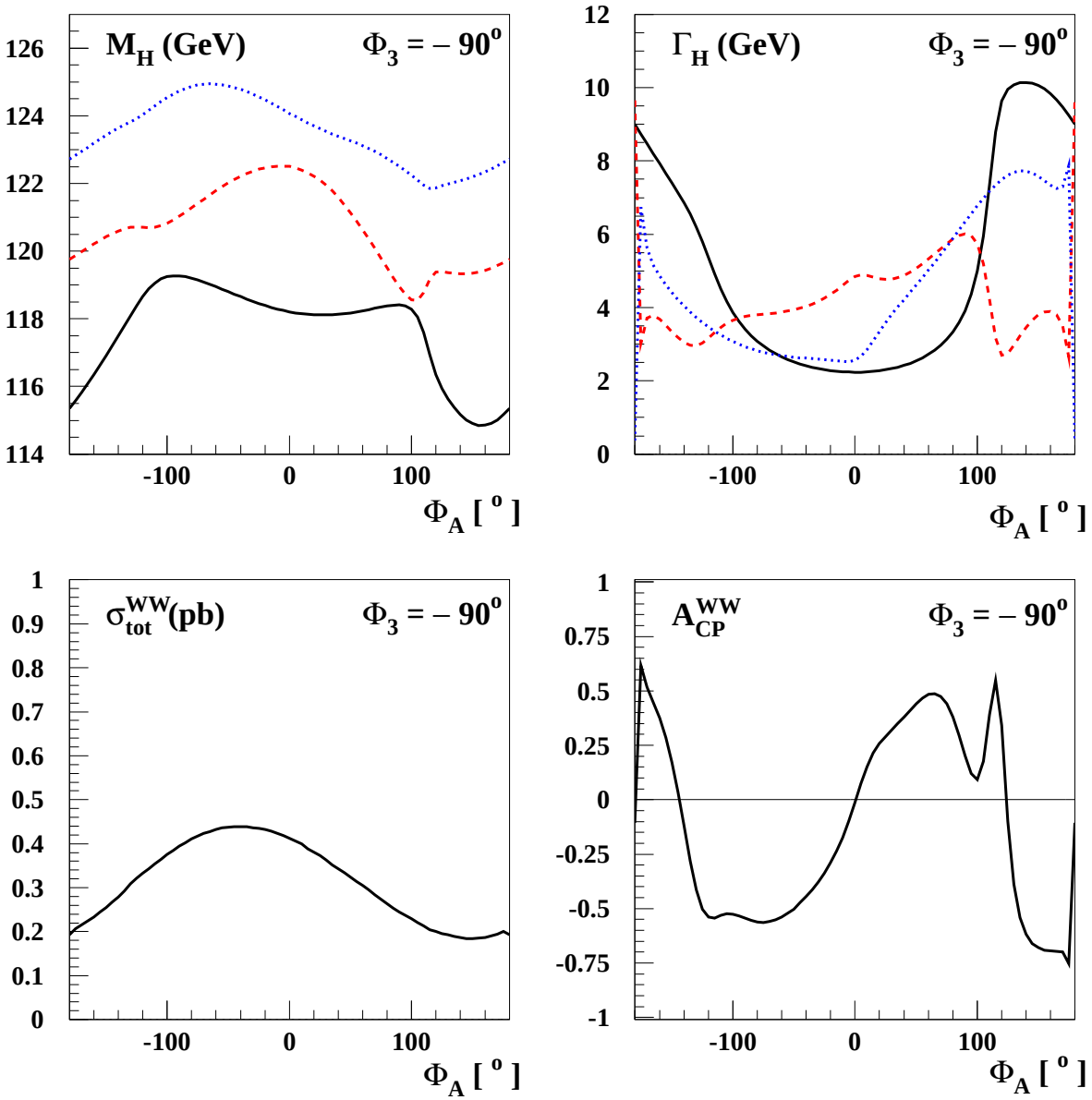

Figure 10: *The same as in Fig. 8, but for* $\Phi_3 = -90°$.

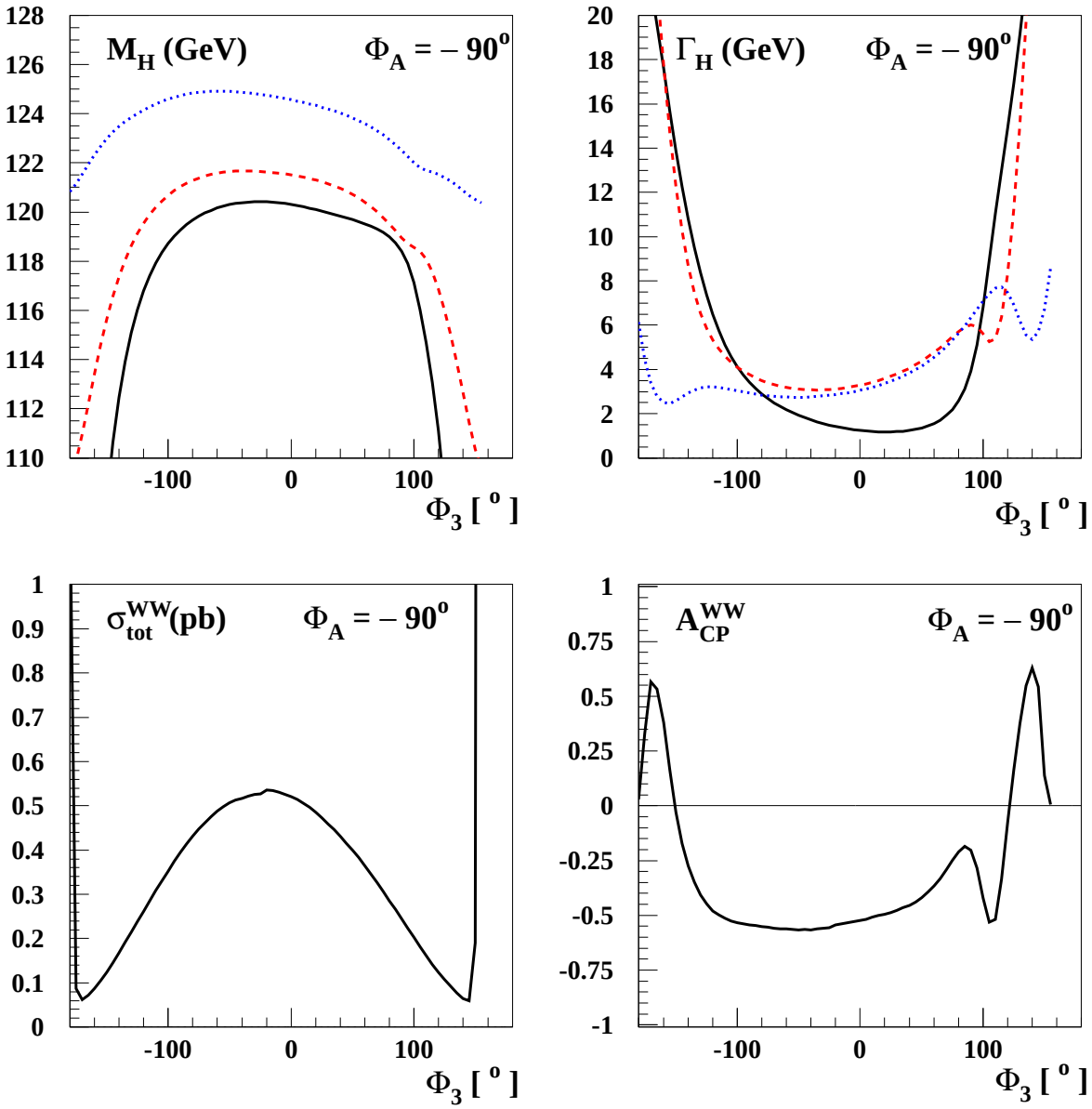

Figure 11: *Numerical values for* $M_{H_{1,2,3}}$ *and* $\Gamma_{H_{1,2,3}}$, $\sigma_{\rm tot}(pp(WW) \to H \to \tau^+\tau^- X)$ *and* $\mathcal{A}_{\rm CP}^{WW}$ *as functions of* Φ_3, *for* $\Phi_A = \Phi_{A_t} = \Phi_{A_b} = \Phi_{A_\tau} = -90°$. *We follow the same line conventions as in Fig. 8.*